AN ECONOMICAL AND SUSTAINABLE DUST SUPPRESSANT FOR GRAVEL ROADS

Final Report
TR-813
July 2025

Sponsored by
The Iowa Department of Transportation

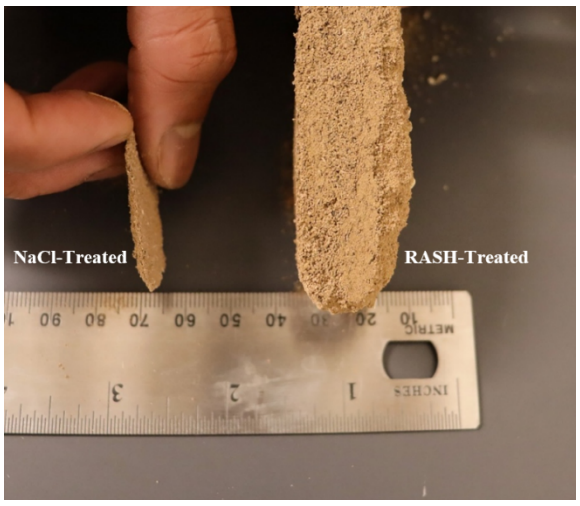

Disclaimer Notice

The contents of this report reflect the views of the authors, who are responsible for the facts and the accuracy of the information presented herein. The opinions, findings, and conclusions expressed in this publication are those of the authors and not necessarily those of the sponsors.

The sponsors assume no liability for the contents or use of the information contained in this document. This report does not constitute a standard, specification, or regulation. The sponsors do not endorse products or manufacturers. Trademarks or manufacturers' names appear in this report only because they are considered essential to the objectives of the document.

Statement of Non-Discrimination

Iowa DOT ensures non-discrimination in all programs and activities in accordance with Title VI of the Civil Rights Act of 1964. Any person who believes that they are being denied participation in a project, being denied benefits of a program, or otherwise being discriminated against because of race, color, national origin, gender, age, or disability, low income and limited English proficiency, or if needs more information or special assistance for persons with disabilities or limited English proficiency, please contact Iowa DOT Civil Rights at 515-239-7970 or by email at civil.rights@iowadot.us.

TECHNICAL REPORT DOCUMENTATION PAGE

1. Report No. IHRB Project TR-813	2. Government Accession No.	3. Recipient's Catalog No.
4. Title and Subtitle TR-813 An Economical and Sustainable Dust Suppressant for Gravel Roads		5. Report Date August 2025
		6. Performing Organization Code
7. Author(s) Ravi Kiran Yellavajjala, Ph.D., P.E. https://orcid.org/0000-0001-8300-0767 Maedeh Hesami, https://orcid.org/0009-0006-2028-2991		8. Performing Organization Report No.
9. Performing Organization Name and Address Arizona State University ISTB-5, 174 Tempe, AZ 58105-5285 Phone: 480-965-2790		10. Work Unit No.
		11. Contract or Grant No.
12. Sponsoring Agency Name and Address Iowa Highway Research Board Iowa Department of Transportation 800 Lincoln Way Ames, IA 50010.		13. Type of Report and Period Covered 6/1/2023-08/21/2025
		14. Sponsoring Agency Code
15. Supplementary Notes		

16. Abstract

Air pollution from fugitive dust poses a significant health risk to the population in rural and arid regions. Conventional chloride-based suppressants offer temporary dust control, leading to soil contamination and infrastructure corrosion. This study proposes the synthesis of a starch-based powder that regenerates into a hydrogel for dust mitigation, owing to its agglomeration and crust-forming abilities. The hydrogel was synthesized by thermally degrading amylopectin-rich starch, undergoing a freeze-thaw cycle, and pulverizing it into powder. The powder was then added to hot water (>65°C) at concentrations of 0.5%, 1%, 2%, and 3% by weight of solution to form regenerated amylopectin starch hydrogel (RASH). Dust suppression performance was evaluated using PI-SWERL (Portable in-situ Wind Erosion Lab) to assess wind erosion rates, and penetration tests to measure crust strength. Results demonstrated that 1%wt. RASH achieved a 100% reduction in wind erosion rates, even at a speed of 90 km/h. This is attributed to the agglomeration of soil grains and the formation of a thick crust. Field tests over 20 days confirmed sustained PM10 suppression in extreme arid conditions (39°C) across various soil types. As a result, a novel, energy-efficient starch-based dust suppressant is proposed, offering a low-cost and scalable solution for long-term dust control in arid climates.

17. Key Words	18. Distribution Statement
Dust control, Unpaved road, Organic polymers, Sodium Chloride, Calcium chloride and Gels	No restrictions.

19. Security Classif. (of this report)	20. Security Classif. (of this page)	21. No. of Pages	22. Price
Unclassified	Unclassified	44	$99,482.00

Form DOT F 1700.7 (8-72) Reproduction of completed page authorized

TR- 813: An Economical and Sustainable Dust Suppressant for Gravel Roads

Final Report
August 2025

Principal Investigator

Ravi Kiran Yellavajjala, Ph.D., P.E.
Associate Professor
School of Sustainable Engineering and the Built Environment
Arizona State University

Co-author

Maedeh Hesami*
*Graduate Research Assistant
School of Sustainable Engineering and the Built Environment
Arizona State University

Sponsored by

the Iowa Highway Research Board
(IHRB Project TR-813)

A Report from

Damage in Materials and Structures Laboratory
School of Sustainable Engineering and the Built Environment
Arizona State University
ISTB-5, 174
Tempe, AZ 58105-5285
Phone: 480-965-2790
https://labs.engineering.asu.edu/dams/

Acknowledgements

We sincerely appreciate the financial support from the Iowa Department of Transportation. We are especially grateful to Vanessa Goetz for her leadership and commitment to this project, which played a crucial role in its successful execution. The guidance and feedback from the Technical Assistance Committee have been instrumental in shaping our work, and we extend our heartfelt thanks to Lee Bjerke, B. Wilkinson, and Todd Kinney for their valuable comments. Additionally, we acknowledge the support of the School of Sustainable Engineering and the Built Environment lab manager, Jeff Long, and Dr. Emmanuel Salifu, for their essential assistance in the experimental phase of this project.

Contents

List of figures

List of Tables

Chapter 1. INTRODUCTION

1.1 Introduction

Air pollution is one of the major environmental threats to human health, fueled by the rapid growth of industrial and technological activities. According to the World Health Organization (WHO), more than 8 million premature deaths each year are linked to air pollution [1,2]. As an important subset of air pollution, dust pollution is driven by emission of fugitive dust particles from different sectors like construction [3–5], agriculture [6,7], mining [8,9], and unpaved roads [10–15]. This type of pollution entrains fine particulate matter, such as PM10 and PM2.5, which are harmful to air quality and are linked to serious health issues [15–17].

In the United States, fugitive dust from unpaved roads and construction sites alone contributes to over 34% of particulate emissions, making it a primary source of airborne particulate matter [19]. The effects of fugitive dust are far-reaching, especially in arid and semi-arid regions, where dry conditions exacerbate dust generation leading to reduced visibility, respiratory problems, waterway pollution, soil degradation, and decreased agricultural productivity [7,12]. Various dust control techniques have been developed to stabilize the top layer of soil and these techniques have one or both of the mechanisms, namely, hygroscopicity, which refers to the ability to absorb and retain moisture, and agglomeration, which involves binding of soil particles [13]. Among these techniques, chemical stabilizers are the most widely adopted in practice due to their ease of application and economic viability [20,21].

Specifically, chloride-based salts, such as calcium chloride ($CaCl_2$) and magnesium chloride ($MgCl_2$), are among the most widely used dust suppressants due to their hygroscopic properties [13]. However, various drawbacks have been reported, including the corrosion of infrastructure and vehicles [22–24], adverse effects on soil health and fertility [25,26], contamination of freshwater resources [27–29], and potential loss of biodiversity [29,30]. As an alternative, bio-based polymeric dust suppressants have gained significant attention due to their environmental friendliness and sustainability [31–34]. Among the most common biopolymers used for soil stabilization are starch [21,35–37], guar gum [38–40], sodium alginate [41–43], crop straw [44,45], and chitosan [37,46,47].

Starch has emerged as a highly promising option due to its abundance, cost-effectiveness, and versatility. Starch is a natural polysaccharide primarily derived from corn, potatoes, and other plant sources, making it readily available and renewable. Its hydrophilic properties allow it to absorb and retain water effectively, while the high viscosity can bind soil particles together and form a stable non-toxic soil-binding matrix [41,48]. To prepare starch-based dust suppressant, several modification methods can be applied to improve binding, water retention, and stability properties. Zhu et al. [35] proposed a starch/organo-bentonite composite liquid dust suppressant (CLDS) by using potato starch, acrylic acid, and sodium bentonite as raw materials through in situ intercalative polymerization. The resulting polymer exhibited a porous three-dimensional network

structure, which formed a protective layer with high viscosity that effectively stabilized soil particles.

Jian Sun et al. [49] proposed an environmentally friendly composite dust suppressant using starch as the base material, with methyl methacrylate and acrylamide as monomers, combined with a surfactant through graft copolymerization. Their results demonstrated an excellent efficiency of over 80% when subjected to wind speeds up to 43 km/h, highlighting the composite's robustness in controlling dust under varying wind conditions. Liang et al. [50] developed a starch-based superabsorbent polymer (SAP) using cassava starch as the base material. The synthesis was carried out through a combination of mechanical activation-assisted solid-phase reaction (MASPR) and conventional liquid-phase (LP) methods. Their results indicated that this approach enhanced the SAP's fluidity and film-forming characteristics, significantly improving its effectiveness as a dust suppressant, even under wind speeds exceeding 43 km/h.

These materials, while effective in laboratory conditions, are not tested in the field extensively. Furthermore, some of these methods require costly raw materials, involved preparation methods which limits their applications. In addition, the long-term performance of these dust suppressants, especially under harsh environmental conditions such as prolonged sunlight exposure and the intense, dry climates found in arid regions is rarely investigated. To address these limitations, it is essential to develop a cost-effective, scalable approach for sustained dust suppression in diverse field conditions.

1.2 Motivation

Effective dust suppression in arid and semi-arid regions remains a challenge, especially where chloride-based agents show limited durability. This study addresses this gap by developing a regenerated amylopectin starch hydrogel (RASH) using a heat-based, energy-efficient synthesis route. Unlike previous chemically cross-linked starch polymers, RASH uses a physically regenerated powder form of starch that transforms into a gel upon contact with hot water. This regeneration eliminates the need for chemical crosslinkers, enabling the use of locally sourced, renewable materials. The performance of RASH is assessed through comprehensive laboratory testing for wind erosion resistance and crust strength, followed by field trials to evaluate real-world applicability and long-term performance under harsh conditions.

1.3 Research Gap

Although bio-based dust suppressants have gained increasing attention as eco-friendly alternatives to chloride-based stabilizers, there remains a significant research gap in developing shelf-stable, sustainable, and field-deployable formulations. Many existing starch-based solutions rely on multi-step chemical modifications, synthetic crosslinkers, or emulsification processes that are not only cost-prohibitive but also difficult to scale for widespread application. These systems are often formulated as liquids or gels with limited shelf life, requiring cold storage or immediate use after preparation, which limits their practicality for remote or large-scale operations. Moreover, the performance of these materials is typically evaluated under idealized laboratory conditions that

do not reflect the complexities of real-world environments. Few studies have investigated how bio-based suppressants perform under prolonged environmental stressors such as extreme heat and direct sunlight, conditions commonly encountered in arid and semi-arid regions where dust generation is most severe. Additionally, while the use of starch as a binder has shown promise, the specific application of physically modified, shelf-stable starch powders that can be easily transported and regenerated into hydrogels on-site with minimal energy and water input remains largely unexplored. This limits the ability to create scalable and on-demand dust suppression solutions using locally available renewable resources.

1.4 Research Objectives

This study aims to fill the identified gap by pursuing the following objectives:

1. To synthesize a powder-form, shelf-stable regenerated starch hydrogel using amylopectin-rich corn starch.
2. To characterize the surface morphology, crust formation, and wind erosion resistance of RASH in laboratory settings.
3. To compare the performance of RASH against conventional chloride-based suppressants and water in reducing PM_{10} emissions.
4. To evaluate the scalability and field performance of RASH through controlled application at two construction sites with different soil types.

1.5 Organization of the Report

The structure of this report is designed to comprehensively present the development and evaluation of a regenerated starch-based hydrogel for dust suppression. Chapter 2 outlines the synthesis methodology of the Regenerated Amylopectin Starch Hydrogel (RASH), including powder preparation, regeneration process, and characterization of hydrogel properties relevant to environmental applications. Chapter 3 describes the laboratory testing procedures employed to assess the dust mitigation potential and surface mechanical behavior of RASH-treated soils using the PI-SWERL device and penetration resistance measurements. Chapter 4 presents the results of field trials conducted in Tempe, Arizona, to evaluate the performance of RASH under real-world environmental conditions, including wind exposure over a 20-day period, with comparisons to conventional salt- and water-based treatments. Chapter 5 concludes the report with a synthesis of the findings, highlights their broader implications, and offers recommendations for future research and implementation strategies.

1.6 Research Products

The following research output has been generated from this study:

1.6.1 Journal Paper

Hesami, M. and Kiran, R., 2025. Starch-based Hydrogel Powder for Enhanced Dust Suppression. *Cleaner Engineering and Technology*, p.101055. https://doi.org/10.1016/j.clet.2025.101055

1.6.2 Patent

Kiran R**,** Hesami M. Dust suppression composition and methods of use thereof. U.S. Provisional Patent Application No. 63/720,101. Filed August 23, 2024.

Chapter 2. Synthesis and Characterization of Bio-based Hydrogel for Dust Mitigation

This chapter presents the synthesis of various bio-based hydrogels formulated for environmentally friendly dust suppressants. Four hydrogel systems were developed using naturally derived polymers: lignin–chitosan hydrogel, hydroxyethyl cellulose (HEC) hydrogel, alkali-treated starch hydrogel, and a regenerated starch-based hydrogel. Each formulation was evaluated based on ease of preparation, environmental compatibility, and suitability for field application.

The initial sections of this chapter describe the materials used and detail the synthesis procedures for each hydrogel type. Following this, a comparative analysis led to the selection of the regenerated amylopectin starch hydrogel (RASH) as the most practical candidate due to its bio-origin, simplicity of regeneration, and shelf stability. The latter part of the chapter focuses exclusively on the regenerated starch hydrogel, outlining the full regeneration protocol and providing comprehensive characterizations. These tests include viscosity and pH measurements, particle size distribution, morphological observation, and elemental analysis to assess the hydrogel's performance and interaction with soil under dust-prone conditions.

2.1 Materials

The materials used in this study included chitosan (medium molecular weight), alkali lignin, hydroxyethyl cellulose (HEC), sodium hydroxide (NaOH), glycerol, and citric acid, all of which were obtained from Sigma-Aldrich. Commercially available corn starch was used as the starch source. Distilled water was used throughout the preparation and testing procedures.

2.2 Synthesis Process of Bio-Based Hydrogels

2.2.1 Lignin-Chitosan Hydrogel

Lignin is a naturally abundant phenolic polymer that serves as a critical structural component in vascular plants. It consists roughly 25% of wood by weight and is mostly discarded or incinerated during the paper pulping process, despite its renewable origin and non-toxic nature [51,52]. Recently, alkali lignin has gained attention as a sustainable and cost-effective ionotropic cross-linker, particularly for chitosan, a biodegradable polysaccharide derived from chitin [53].

In this study, lignin–chitosan hydrogels were synthesized through ionotropic gelation, where the electrostatic interaction between the negatively charged phenoxide groups in lignin and the positively charged ammonium groups on the chitosan backbone led to the formation of a cross-linked network. A similar strategy has been previously applied in biomedical applications for wound care [54]; however, the method was modified here to ensure compatibility with soil environments. To adjust the pH for soil health, sodium hydroxide (NaOH) was introduced during the synthesis process.

The hydrogel was prepared by dissolving 3 grams of chitosan in 300 milliliters of 3% acetic acid and stirring the mixture for about 10 minutes. Separately, 2 grams of alkali lignin were dissolved in 200 milliliters of distilled water and gradually added to the chitosan solution with continuous stirring. Following this, 100 milliliters of 0.1 M NaOH were added to initiate gelation and bring the pH closer to neutral. The pH of the resulting hydrogel was 4.78 using an Oakton PH 550 pH Meter. The gels were directly used as a bio-based dust suppressant.

2.2.2 Hydroxyethyl Cellulose (HEC) Hydrogel

Hydroxyethyl cellulose (HEC) is a water-soluble, non-ionic polymer derived from cellulose, commonly used for its thickening, film-forming, and stabilizing properties. It's known for being safe, biodegradable, and compatible with a wide range of formulations [39,55]. In this work, a simple heating method was used to prepare a hydrogel from HEC without the need for any additional cross-linkers or chemical modifications.

To form the gel, 5 grams of HEC powder were dissolved in 500 milliliters of deionized water to make a 1% (w/v) solution. The solution was then heated for 10 minutes at 35°C while being stirred continuously. During heating, the initially clear and viscous solution gradually thickened and took on a soft gel-like consistency. Heating helps disrupt the existing hydrogen bonds within and between HEC molecules, allowing the chains to move more freely and interact with surrounding water molecules. As the solution cools or stabilizes at the new temperature, the polymer chains begin to re-associate through hydrogen bonding and entanglement. These physical interactions give rise to a three-dimensional network that traps water and holds the gel structure together. Since no chemical reaction takes place, this process is considered reversible and driven purely by physical forces. The final pH of this hydrogel was 7.85 as shown in Table 2-1. The resultant hydrogel can be directly applied on soil surface as a dust suppressant.

2.2.3 Alkali-treated starch

This section proposed a room-temperature gelatinization method for starch using an alkaline system composed of sodium hydroxide (NaOH) and glycerol. Alkaline treatment is known to break the hydrogen bonds within and between starch molecules, which helps the starch granules swell and dissolve more easily [56]. While starch typically requires heat to gelatinize, previous studies have shown that certain chemical combinations can achieve similar results at room temperature. In this case, glycerol played an important role as a plasticizer, helping to prevent the starch chains from clumping back together once they're separated, which is a common issue known as retrogradation.

To prepare the hydrogel, 2 grams of starch were added to 98 milliliters of water, creating a 2% solution. Then, 1.5 grams of NaOH and 1 gram of glycerol were introduced, and the mixture was stirred continuously for 45 minutes. As the solution became more viscous, indicating gelatinization, 2 grams of citric acid were added to neutralize the pH, followed by another 5 minutes of stirring to ensure uniformity. The final pH was recorded as 6.95. The ease of preparation, biodegradability, and compatibility with soil make this hydrogel as a strong candidate

for use in sustainable environmental solutions. A summary of the key properties of the three synthesized hydrogels is provided in Table 2-1, and their visual appearance is shown in Figure 2-1.

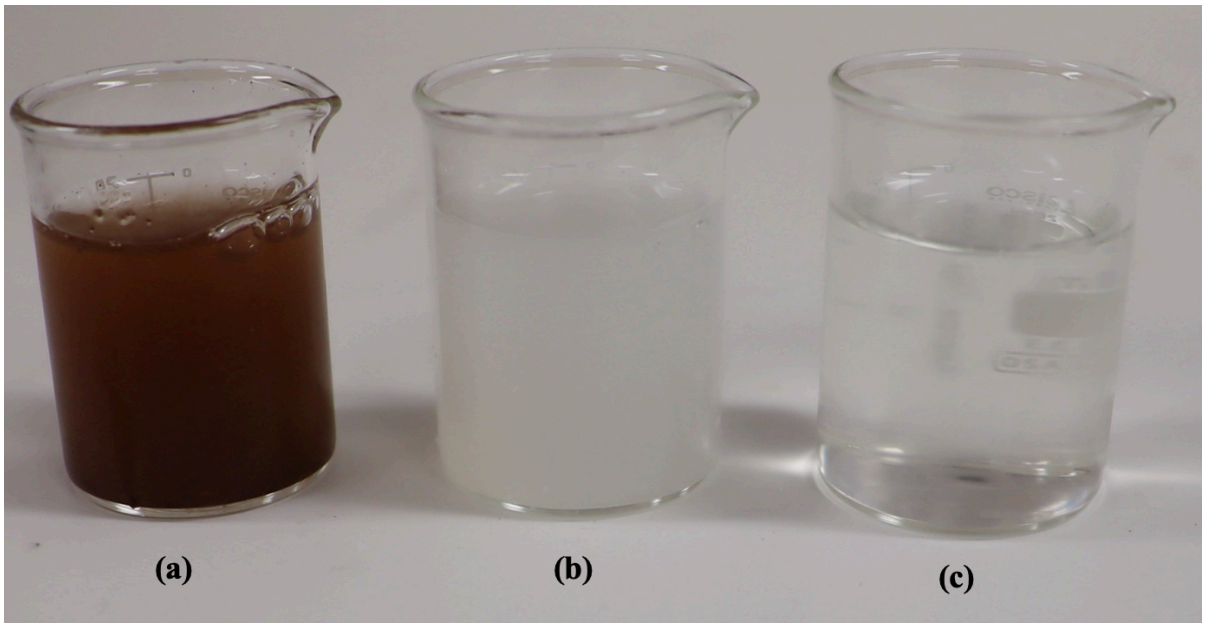

Figure 2-1. Visual appearance of hydrogel solutions prior to application (a)Lignin-Chitosan hydrogel (HA), Hydroxyethyl cellulose (HB), and Alkali-treated starch (HC)

Table 2-1. Summary of synthesized hydrogels in this study

Commercial Name	Hydrogel Name	Base Materials	Mechanism	pH
HA	Lignin-Chitosan Hydrogel	Chitosan , Alkali Lignin	Electrostatic interaction (ionotropic association)	4.78
HB	HEC Hydrogel	Hydroxyethyl Cellulose	Physical gelation via H-bonding and entanglement	7.85
HC	Alkali-treated Starch	Starch , NaOH	Alkaline disruption of H-bonds and chain relaxation	6.95

2.2.4 Regenerated Starch Hydrogel

Amylopectin-rich corn starch powder (90% amylopectin) and normal corn starch powder (70% amylopectin) were procured. Corn starch consists primarily of two glucose polymers: amylose and amylopectin . Amylopectin is a highly branched polysaccharide with α-1,4 linked glucose units and α-1,6 linkages at branch points. The water absorption capacity and mechanical properties of corn-based hydrogels are influenced by the relative amounts of amorphous and crystalline amylopectin. A higher proportion of amylopectin was found to enhance water absorption [57]. For this reason, amylopectin-rich corn starch, containing approximately 90%

amylopectin, was used, while normal corn starch, which consists of around 70% amylopectin, was employed for comparative analysis.

2.2.4.1 Synthesis process of hydrogel

The synthesis of the hydrogel powder involved three main stages: thermal gelatinization, structural stabilization, and hydrogel regeneration. Each step is described in detail in the following subsections

2.2.4.2 Thermal gelatinization process

5% by wt. corn starch solution was prepared by suspending "X" grams of corn starch (amylopectin-rich and normal) in 19X mL of distilled water. The mixture was magnetically stirred for 15 minutes at 90°C. During heating, starch gelatinization was initiated as amorphous regions hydrate, causing starch granules to swell and amylose molecules to leach out. This intense expansion imposed stress on crystalline domains, ultimately leading to the disruption of crystallites and the release of amylopectin [58]. At this stage, the starch exhibited gel-like properties, as water became entrapped within swollen granules, forming a semi-solid matrix.

2.2.4.3 Structural stabilization

Following the gelatinization phase, retrogradation occurred as the starch solution was cooled to room temperature, initiating the re-crystallization of amylose and amylopectin chains. This retrogradation process began stabilizing the gel structure by forming hydrogen bonds, making the starch matrix firmer and less susceptible to breakdown [59]. The solution then underwent a freeze-thaw cycle, where it was frozen at -18°C for 24 hours and subsequently thawed to room temperature. This cycle promoted further phase separation and polymer chain reorganization, expelled excess water from the gel matrix, and enhanced structural stability [60]. After a 48-hour thawing period, the foam-like structure was ground into a fine powder. Figure 2-2 illustrates the granular morphology of amylopectin corn starch powder before and after treatment using a Keyence VHX-7000 optical microscope. The raw amylopectin powder, originally consisting of smaller spherical granules, transformed into angular grains post-treatment. This morphological change increased the surface area, leading to enhanced water penetration [58], improved solubility [59], and accelerated hydrogel regeneration [61]. Similarly, Figure 2-3 presents the granular morphology of untreated and treated normal corn starch powder. Like amylopectin, the spherical morphology of the untreated starch transitioned to an angular structure post-treatment. The regenerated powders exhibited clear disruptions in granule integrity due to the physical treatment processes.

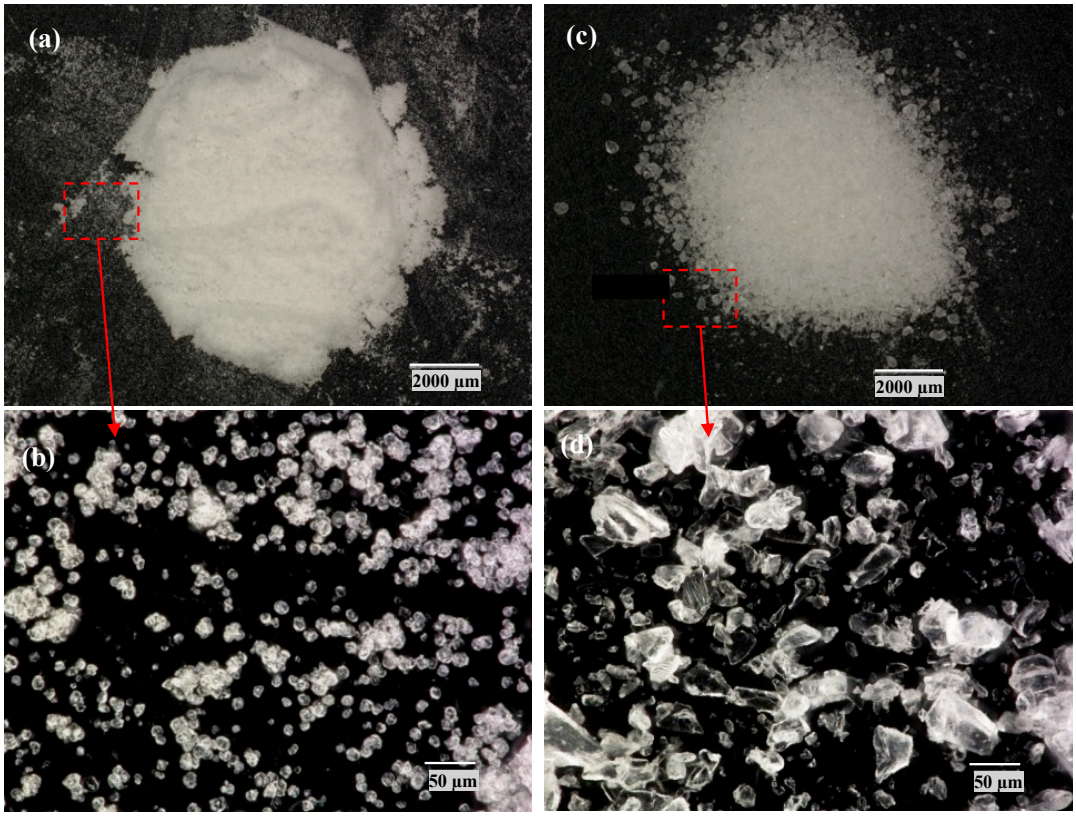

Figure 2-2. Granular morphology of a) raw amylopectin-rich corn starch powder (2000 µm), b) raw amylopectin-rich corn starch powder (50 µm), c) regenerated amylopectin corn starch powder (2000 µm), d) regenerated amylopectin corn starch powder (50 µm).

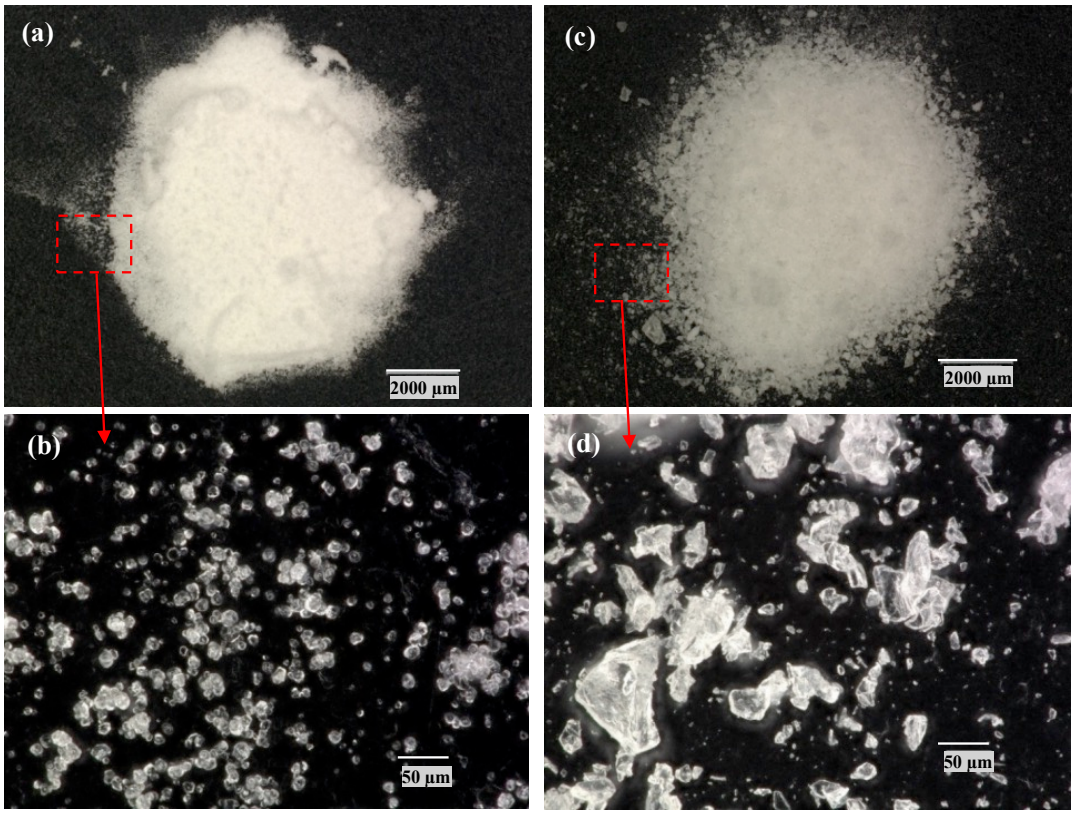

Figure 2-3. Granular morphology of a) raw normal corn starch powder (2000 µm), b) raw normal corn starch powder (50 µm), c) regenerated normal corn starch powder (2000 µm), d) regenerated normal corn starch powder (50 µm).

2.2.4.4 Hydrogel regeneration process

The resultant powder was introduced into warm water (>65°C) to regenerate hydrogels for dust suppression. Different concentrations of regenerated amylopectin starch hydrogel (RASH), ranging from 0.5% to 3% by weight, were used to assess dust suppression efficiency, as shown in Table 2-2. Figure 2-4 shows the regenerated amylopectin starch hydrogel (RASH) and regenerated normal starch hydrogel (RNSH), both at a 1% by weight. Upon regeneration, the RASH formed a homogeneous hydrogel, while the RNSH exhibited insoluble particles. The high amylopectin content in RASH enabled full dissolution in water, resulting in a stable and uniform mixture. In contrast, RNSH exhibited partial solubility due to its higher amylose content [62], resulting in phase separation and a less consistent solution.

Table 2-2. Composition of regenerated amylopectin starch hydrogel (RASH) at various concentrations for dust suppression.

Solutions	0.5%wt. RASH	1%wt. RASH	2%wt. RASH	3% wt. RASH
Regenerated powder (g)	0.5X	1X	2X	3X
Distilled water (g)	99.5X	99X	98X	97X

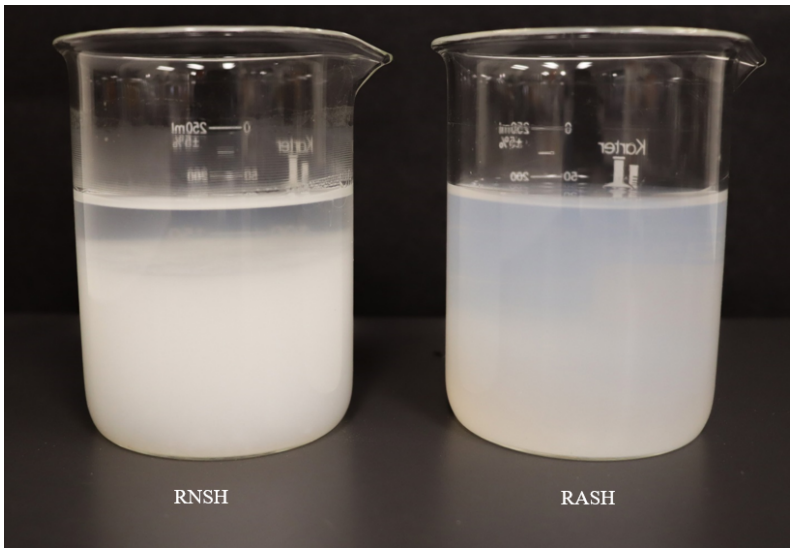

Figure 2-4. Regenerated normal starch hydrogel (RNSH), and regenerated amylopectin starch hydrogel (RASH)

Figure 2-5 illustrates the preliminary application of these hydrogels on the soil surface. The RNSH developed a laminar, layered structure that detached from the soil, rendering it ineffective for dust suppression (see Figure 2-5. a). In contrast, the RASH formed a stable crust that fully integrated with the soil, making it a more reliable candidate for dust suppression. Consequently, RNSH was determined to be unsuitable and excluded from further investigation.

(a) **(b)**

Figure 2-5. Appearance of dried treated surface by a) regenerated normal starch hydrogel (RNSH), b) regenerated amylopectin starch hydrogel (RASH)

2.3 Characterization methods for regenerated hydrogels

Among the synthesized hydrogels evaluated in this study, the regenerated amylopectin-rich starch hydrogel (RASH) was selected for further investigation due to its practical advantages. Unlike the lignin–chitosan, HEC hydrogels, or Alkali-Activated starch, which require synthetic chemicals, chemical reactions, or external heating, the regenerated starch hydrogel is prepared

from bio-based, non-toxic materials using a simple regeneration process. Its powdered form is shelf-stable and can be regenerated in warm water directly in the field without the need for specialized equipment or thermal treatment. These attributes make RASH particularly suitable for scalable and sustainable dust suppression applications. Therefore, the following characterization tests were conducted exclusively on this hydrogel. This section presents the characterization techniques used to evaluate the physical and chemical properties of the regenerated hydrogels and their interaction with soil. The methods include viscosity and pH measurements, particle size analysis, microstructural observation, and elemental composition analysis.

2.3.1 Viscosity and pH Measurements

Viscosity is an important attribute of RASH, as it helps forming a protective crust that resist wind erosion. However, excessively high viscosity can hinder the ease of application when spraying the dust suppressant [21]. It is crucial to select a dust suppressant with a viscosity that balances effectiveness with practicality. The viscosity values of RASH at varying concentrations (0.5%, 1%, 2%, and 3% wt. RASH) were measured using DHR-2, TA Instruments rheometer. Each viscosity measurement was conducted at a constant temperature of 25°C and repeated three times to ensure accuracy and obtain reliable average values. In addition to viscosity, the pH of the hydrogel was measured using the Oakton pH meter. Maintaining the pH of the dust suppressant within a range that is compatible with the soil is essential, as it can influence both the effectiveness of the suppressant and the health of the soil ecosystem [63]. The optimal pH range for soil is typically between 6.0 and 7.5, where nutrient availability is maximized, and microbial activity is preserved [64].

The results of the viscosity and pH tests are summarized in Table 2-3. The pH values for all concentrations of hydrogel maintained a suitable range for soil health [65]. The analysis revealed a direct correlation between the hydrogel concentration and its viscosity. As the concentration increased, the viscosity of the hydrogel also rose significantly. While higher viscosities can enhance the effectiveness of dust suppression by improving wind erosion resistance, excessively high viscosity can pose practical challenges [21]. The application of the 3% wt. RASH was noted to require more energy during spraying, making it less convenient for field applications. Selecting regenerated hydrogel concentrations requires a balance between achieving effective viscosity for dust suppression and maintaining ease of application.

Table 2-3. Viscosity and pH measurements of RASH at varying concentrations.

Wt. of RASH	0.5% wt.	1% wt.	2% wt.	3% wt.
Viscosity (Pa·s)	1.30E-03	2.15E-03	5.81E-02	2.95E-01
pH	6.77	6.78	6.88	6.92

2.3.2 Particle size distribution

Particle size distribution was assessed for both the regenerated hydrogel powder and the in-lab soil. Optical microscopy was used for the hydrogel powder, while soil particle sizes were determined using the sieve method.

2.3.2.1 Particle size distribution by optical microscopy

The particle size of the regenerated hydrogel powder was measured using a Keyence VHX-7000 optical microscope, analyzing 534 particles. As shown in Figure 2-6, more than 40% of the particles fall within the 100-200 μm range, indicating a relatively fine and consistent powder. This size distribution is beneficial, offering enhanced solubility and minimizing the risk of agglomeration, a common issue with smaller particles of raw amylopectin-rich powder (<50 μm) [66].

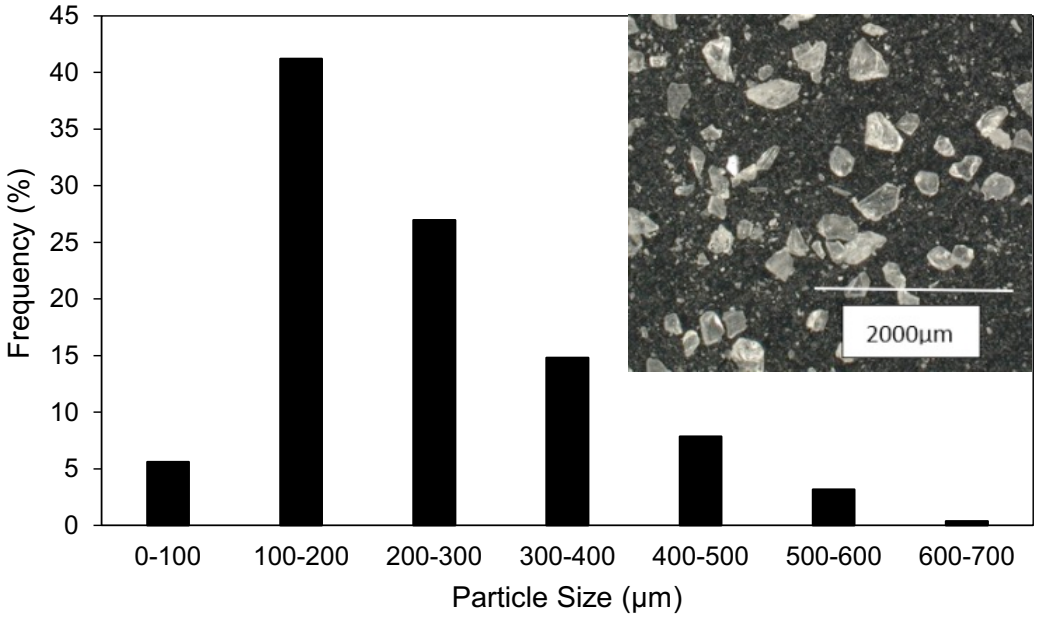

Figure 2-6. Particle size distribution of pulverized regenerated amylopectin starch crystal.

2.3.2.2 Particle size distribution by sieve method

Soil samples were collected from a local site, Vertuccio Farms in Mesa, Arizona, referred to as AZ soil. The collected soil was dried in an electric oven at 50°C to eliminate residual moisture. Then, the soil was sieved using a U.S. Standard 200 mesh (with an opening size of less than 75 μm) to remove any coarser particles, plant debris, or other larger contaminants. The grain size distribution of the soil is depicted in Figure 2-7. As per the Unified Soil Classification System (USCS)[67], AZ soil falls under the classification of silty sand. The detailed results of the sieve analysis are summarized in Table 2-4.

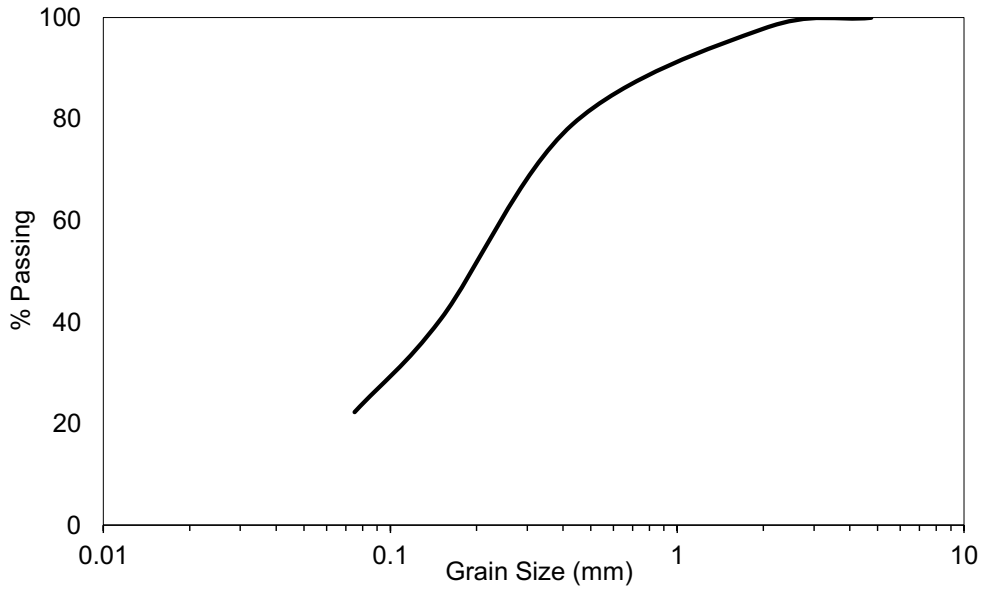

Figure 2-7. Particle size distribution of AZ soil used for in-lab tests.

The AZ soil was selected for testing due to its particle size distribution, which aligns with the size range most susceptible to wind erosion that is fine sand to coarse silt. Larger particles have greater resistance to wind erosion due to their higher mass, whereas smaller particles are more easily displaced. However, the introduction of moisture enhances the erosion resistance of finer particles by binding them together, while silt and clay-sized particles exhibit inter-particle cohesion due to van der Waals forces. These forces cause cations in the pore water to bond with ionic charges on the particle surfaces, increasing cohesion [66]. The Arizona silty sand, with a median particle size (D50) of 0.22 mm (Table 2-4), falls within the size range most susceptible to dust emission [66].

Table 2-4. Results of sieve analysis for AZ soil

Gravel (%)	Sand (%)	Fines (%)	D50(mm)	Coefficient of Uniformity (C_u)	Coefficient of Curvature (C_c)
0.00	77.71	22.29	0.22	7.44	0.99

2.3.3 Morphological analysis

The surface morphology of the treated dust samples was assessed using Keyence Optical Microscopy (VHX-7000). Samples treated with 1% wt. RASH, 10% wt. NaCl, and distilled water were prepared by evenly spraying each solution onto 50.00 g of AZ soil. After air drying under ambient conditions, the microstructural features were evaluated at varying magnifications using Depth-from-Defocus (DFD) technology. This approach allowed for high-precision imaging, capturing detailed surface features and height variations across the samples [68].

Figure 2-8 illustrates the surface morphology of dust samples treated with distilled water, 10% wt. NaCl, and 1% wt. RASH, captured at 250 µm, 50 µm, and 25 µm scales. The surface treated with distilled water (Figure 2-8.a-c) revealed insufficient soil particle binding, with notable

pores between particles. This lack of binding creates a vulnerable surface, as water alone does not contribute to the sustained cohesion of soil particles. In the 10% wt. NaCl-treated sample (Figure 2-8. d-f), a layer of crystallized salt was observed, filling some of the spaces between particles. Despite this, the surface exhibited significant porosity, leading to a brittle crust. While NaCl aids in moisture retention, it fails to provide the structural integrity required for long-term dust suppression, making the surface susceptible to wind erosion. The regenerated hydrogel, on the other hand, formed a solidified film that tightly agglomerated particles of different sizes, resulting in a compact and agglomerated structure. The incorporation of RASH elevated viscosity, caused the agglomeration of soil particles. This binding mechanism created a more robust surface, capable of withstanding wind-induced erosion while significantly extending the dust suppression effect. This mechanism is further supported by the cross-sectional microscopic image shown in Figure 2-9, where the regenerated hydrogel visibly binds adjacent soil particles into a consolidated crust.

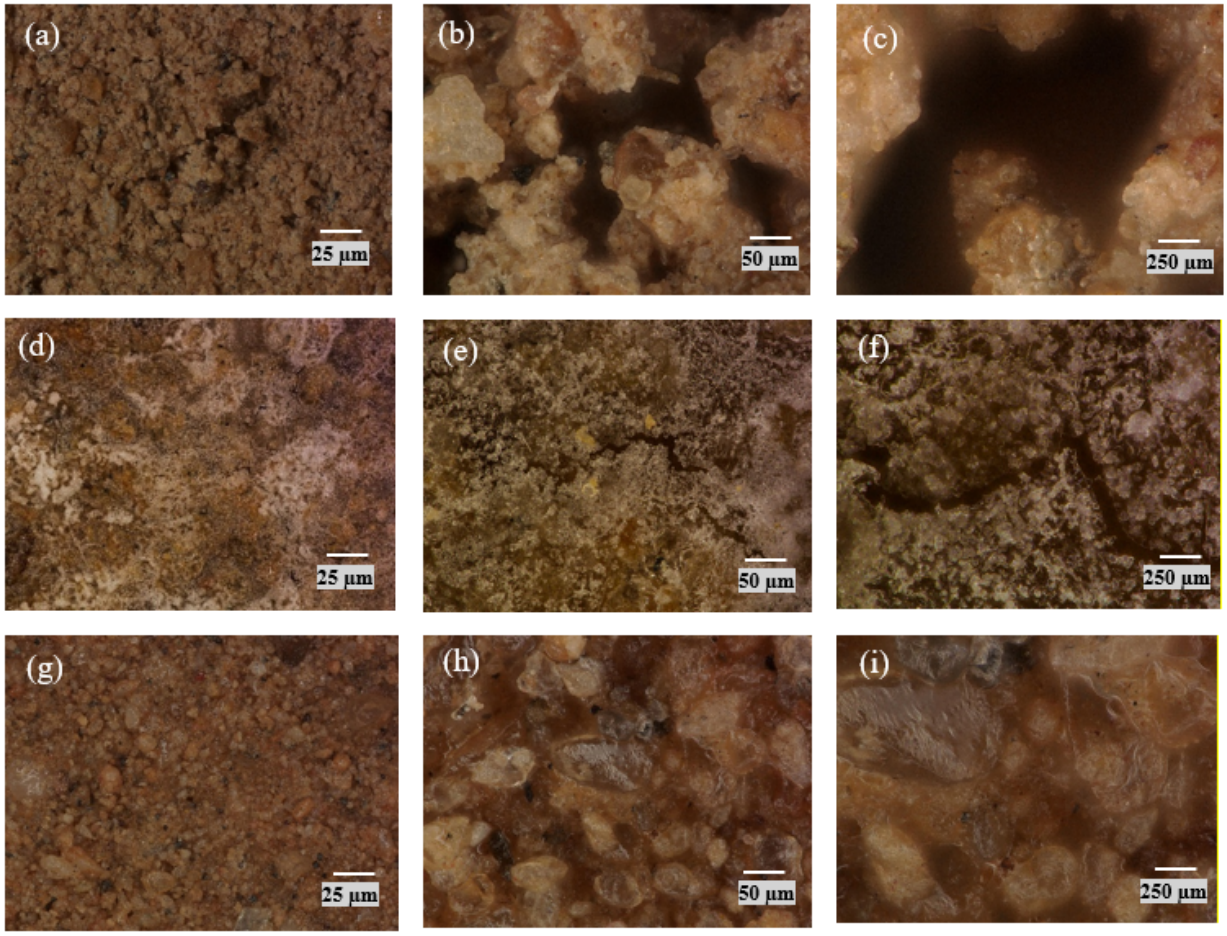

Figure 2-8. Microstructural analysis of surface morphology for dust samples treated with: a-c) distilled water at 25 µm, 50 µm, and 250 µm scales, d-f) 10%wt. NaCl brine solution at 25 µm, 50 µm, and 250 µm scales, and g-i) 1%wt. RASH at 25 µm, 50 µm, and 250 µm scales.

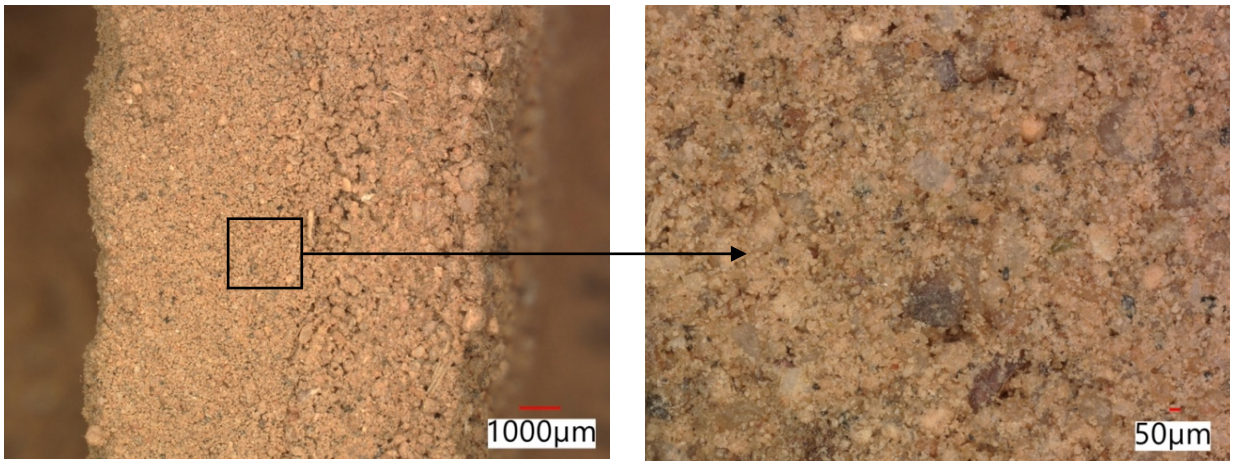

(a) (b)

Figure 2-9. Microstructural cross-section of 1% wt. RASH treated soil (a) at 1000 µm scale, (b) magnified image highlighting particle binding at 50 µm scale.

2.3.4 Elemental analysis

Laser Induced Breakdown Spectroscopy (LIBS) was employed to determine the elemental composition of the dust samples treated with the RASH dust suppressant. LIBS is a technique for in-situ, non-destructive, and multi-element analysis, ideal for material and surface diagnostics. By directing a high-intensity pulsed laser onto the sample, LIBS generates a plasma, and the resulting emission is spectrally analyzed to determine the elemental composition of the material [69]. One of the key benefits of LIBS is its ability to perform depth profiling by drilling into the material without requiring complex sample preparation. This feature makes it well-suited for the analysis of both surface and subsurface regions.

Figure 2-10 illustrates the elemental composition of 1%wt. RASH-treated dust, examined at six different locations on the surface. The analysis predominantly detected elements, including oxygen, carbon, and hydrogen, which are the essential components of organic compounds found in corn starch. The presence of these elements confirms the formation of a crust rich in dried hydrogel on the dust particles. In addition, trace amounts of silicon (Si), potassium (K), and iron (Fe) were also detected, which are commonly found in natural soils [70]. No toxic heavy metals were detected on the treated surface, confirming the environmentally friendly nature of RASH.

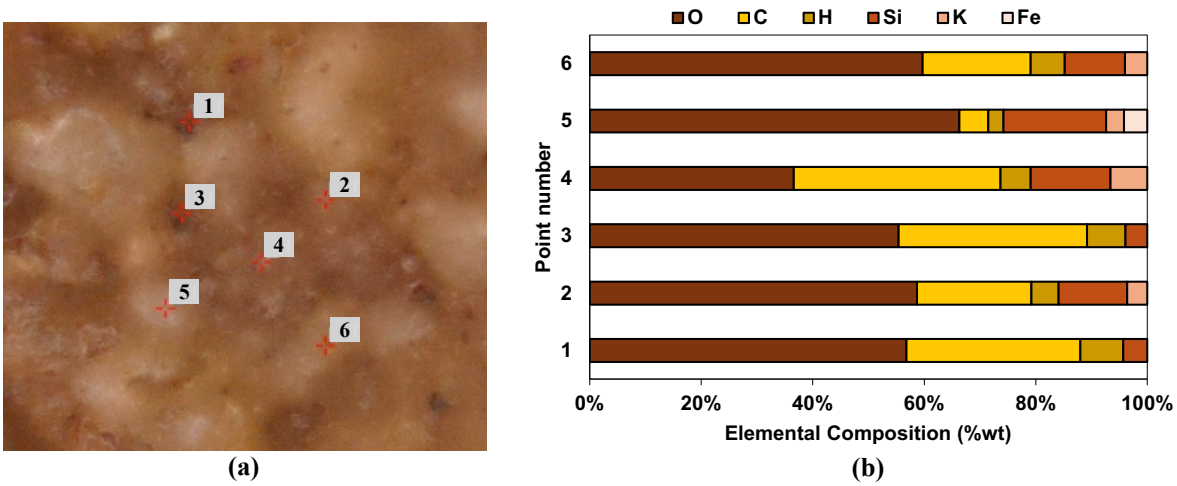

Figure 2-10. Surface elemental composition of 1% wt. RASH-treated dust samples analyzed via Laser Induced Breakdown Spectroscopy (LIBS) at six locations.

The depth profiling technique in LIBS involves irradiating multiple laser pulses at the same position on the surface of the target, allowing for the analysis of elemental composition along the depth direction from the surface to the interior [71]. RASH-treated and untreated dust samples were subjected to a drilling mode for depth profiling, resulting in ten layers with an approximate depth of 10 micrometers for each layer. Figure 2-11.a and Figure 2-11.b present the results of the elemental composition analysis for untreated and 1% wt. RASH-treated samples, respectively. A significantly higher concentration of carbon and hydrogen was found within the first four layers of the treated samples. This observation is attributed to the effective penetration of the RASH into the soil.

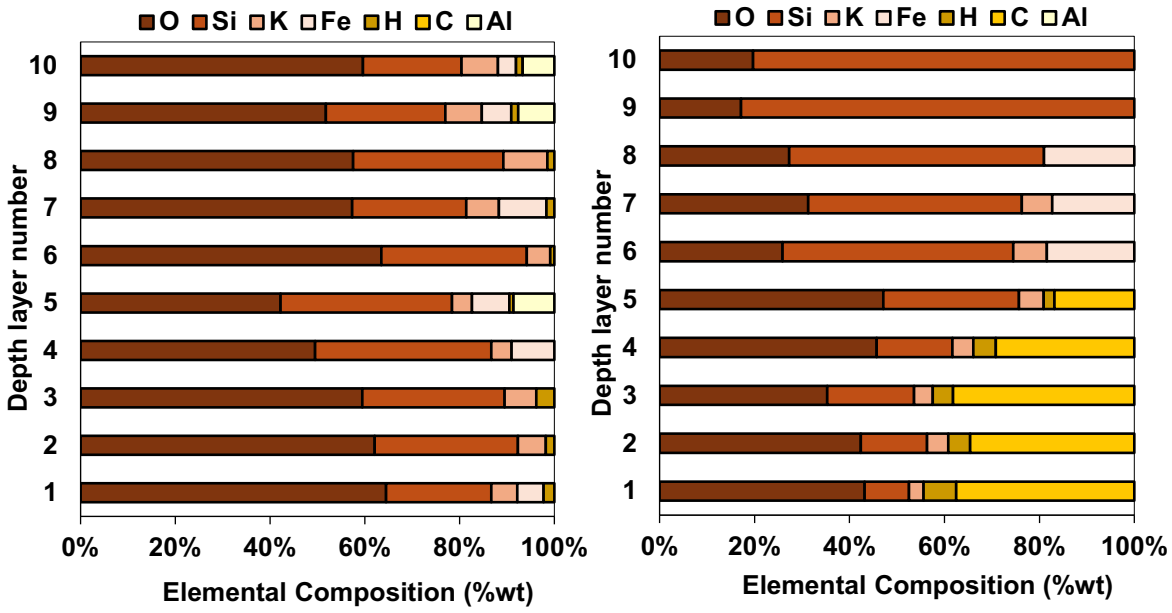

Figure 2-11. Elemental composition (%wt) across sequential depth layers after drilling in Laser Induced Breakdown Spectroscopy (LIBS) analysis: (a) untreated dust sample, (b) 1% wt. RASH-treated dust sample.

2.4 Conclusions

This chapter focused on the synthesis, evaluation, and selection of bio-based hydrogels for dust suppression applications. The following are the main conclusions drawn from this study:

1. Among the four synthesized hydrogels (Lignin–Chitosan (HA), Hydroxyethyl Cellulose (HB), Alkali-Treated Starch (HC), and Regenerated Starch Hydrogel (RASH)), the regenerated amylopectin starch hydrogel was selected due to its simple regeneration process, bio-based composition, and shelf-stable powdered form suitable for field application.
2. RASH was prepared through a thermal gelatinization–retrogradation–freeze-thaw cycle followed by pulverization. Upon mixing with warm water, it formed a homogeneous and stable hydrogel, unlike the normal starch-based counterpart, which exhibited phase separation and incomplete dissolution.
3. Viscosity and pH measurements revealed that RASH maintains soil-compatible pH values (6.77–6.92) across concentrations and shows a direct correlation between hydrogel concentration and viscosity, impacting sprayability and field usability.
4. Microscopic surface analysis showed that RASH-treated soil formed a compact, cohesive crust with minimal porosity and strong particle binding. In contrast, NaCl and water-treated samples displayed weak or brittle structures prone to erosion.
5. Elemental analysis using LIBS confirmed that RASH contributed organic-rich surface layers composed mainly of carbon, hydrogen, and oxygen, and showed no signs of toxic heavy

metals. Depth profiling further demonstrated hydrogel penetration into the top layers of soil, supporting effective dust control performance.

Chapter 3. In-Lab Assessment of Dust Suppression Performance and Surface Crust Strength

This chapter investigates the wind erosion resistance and mechanical stability of soil treated with regenerated starch hydrogel (RASH) through controlled laboratory testing. The aim is to assess the effectiveness of RASH as a sustainable and field-deployable dust suppressant compared to traditional methods such as water or salt application. To quantify airborne dust emissions, the Portable In-situ Wind Erosion Lab (PI-SWERL) was employed. This compact and field-ready device allows for the controlled application of wind shear while measuring particulate matter (PM_{10}) emissions.

Soil samples treated with different concentrations of RASH (0.5–3% wt.) were evaluated alongside water- and salt-treated controls. Key performance indicators such as threshold detachment velocity and PM_{10} concentrations were used to quantify dust suppression efficiency. In addition to wind erosion testing, the mechanical strength of the treated soil surface was assessed using a flat-nose penetration test to measure crust strength. Crust thickness was also measured to evaluate the durability and uniformity of the protective layer formed by the hydrogel.

3.1 In-lab Wind Erosion test

Wind erosion poses substantial environmental challenges, particularly in regions with exposed soil such as construction sites and unpaved roads. A major concern is PM10 which is strictly regulated under national ambient air quality standards due to its adverse effects on human health and the environment [16].

Traditionally, wind tunnels were used as the standard method for assessing dust emissions by simulating atmospheric boundary conditions. However, their large size, complexity, need for flat terrain, and extensive labor make field deployment challenging. To overcome these limitations, the Portable in-situ Wind Erosion Lab (PI-SWERL) was utilized in this study as a reliable method and is shown in Figure 3-1. Unlike traditional wind tunnels, the PI-SWERL is compact and easy to deploy, allowing for rapid and cost-effective dust emission measurements in both laboratory and field environments [72]. The PI-SWERL operates by placing an open-bottom chamber over the soil, where a rotating annular ring applies controlled wind shear. It measures larger particles using optical sensors, while a DustTrak™ sensor monitors the concentration of smaller dust particles, including PM10 [66]. The test utilizes a series of cycles with increasing wind shear levels up to the device's limit, as shown in Figure 3-2. The wind shear in the PI-SWERL test is applied in an annular manner, which is quantified in terms of friction velocity of the wind on the soil surface according to the following equation

$$u_* = C_1 \alpha^4 (RPM)^{\frac{C_2}{\alpha}} \quad (1)$$

where C_1 and C_2 are constants, α is the surface roughness factor, and RPM is the rotating speed of the annular blade in rotations per minute [66].

Figure 3-1. Portable in-situ Wind Erosion Lab (PI-SWERL) test device.

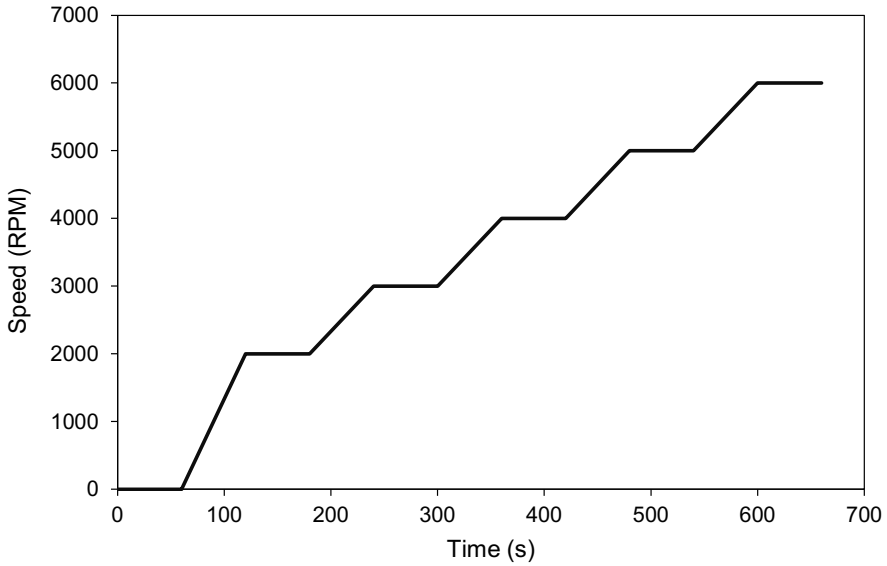

Figure 3-2. Wind speed in PI-SWERL test setup.

The samples of water-treated (wet control and dry control), salt-treated, and RASH-treated were prepared in commercial round pans with a diameter of 22.9 cm and a depth of 3.8 cm. To evaluate the ideal concentration of the RASH, various weight concentrations of 0.5%, 1%, 2%, and 3% (wt. RASH powder) were utilized as dust suppressants. PI-SWERL testing was conducted on the samples 48 hours after the initial application of the various dust suppressants, excluding the wet control. For the wet control, the PI-SWERL test was performed immediately after application while the surface was wet. A surface roughness factor of 0.98 was assumed for the treated soil surfaces, following the guidelines [73]. Figure 3-3 illustrates the PM10 concentration at varying wind velocities, comparing the dust suppression performance of salt-treated samples against the control, 48 hours after application. The threshold detachment velocity, defined as the velocity at which a rapid rise in PM10 concentration is first observed, was approximately 42.2 km/h for salt-

treated samples and 37.8 km/h for water-treated samples (see Figure 3-3). The higher detachment velocity of the salt-treated samples indicates enhanced resistance to dust emission compared to the untreated control [66].

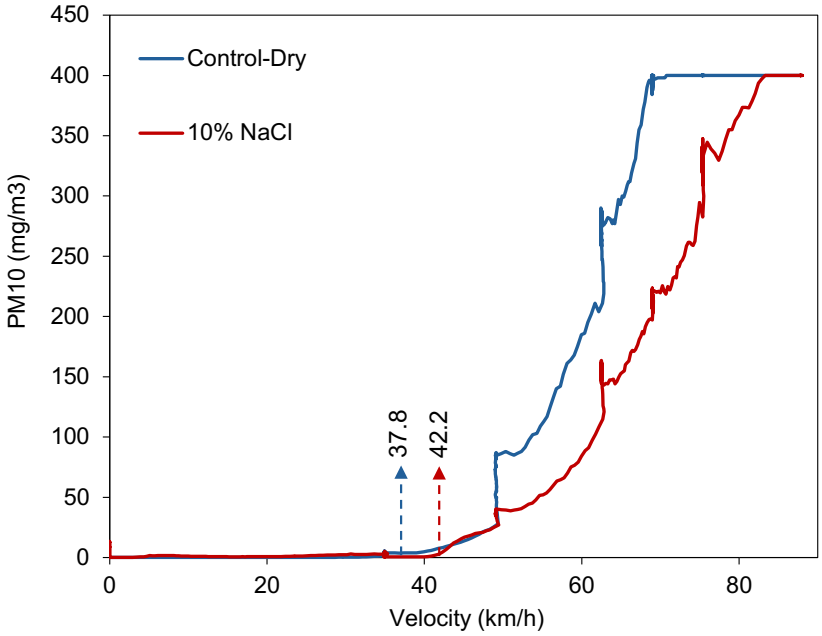

Figure 3-3. Concentration of particulate matter (PM10) for salt-treated and water-treated samples in varying wind velocities.

To assess the efficiency of varying weight concentrations of RASH-treated samples, Figure 3-4 presents a comparison among the most effective treatments. The results reveal that the 1%wt. and 2%wt. RASH concentrations demonstrated superior performance, exhibiting minimal particle detachment from the surface tested (threshold detachment velocity > 90 km/h) and outpacing the performance of the control wet solution. Notably, RASH-treated samples were evaluated 48 hours after drying, while the wet control was tested immediately after application, highlighting the efficiency of the RASH treatment.

In addition to performance trends, visual inspection after drying revealed that higher concentrations of RASH (3% wt.) tended to exhibit localized drying shrinkage and visible cracks. Figure 3-5 compares 1% and 3% RASH-treated surfaces, highlighting the crack formation at higher concentrations. The increased viscosity of higher RASH percentages made the spraying process more challenging, impacting uniform application.

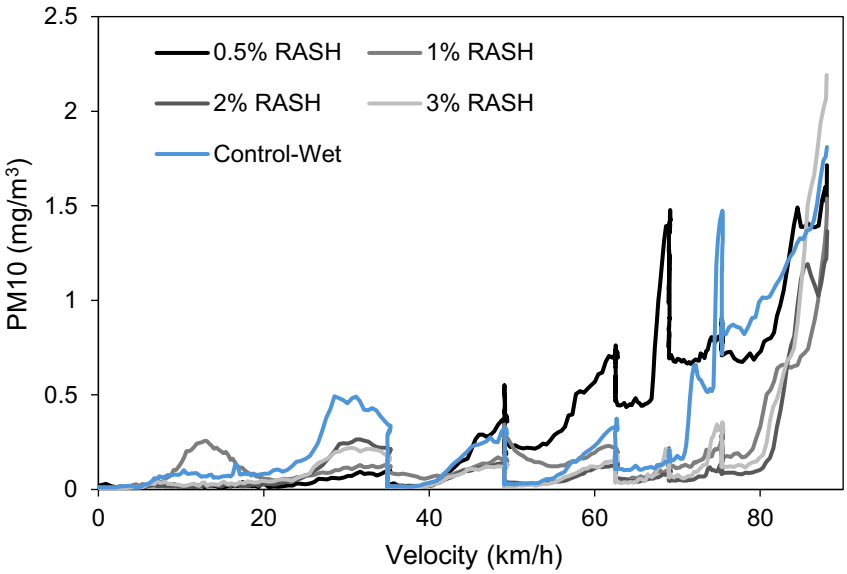

Figure 3-4 . Concentration of particulate matter (PM-10) relative to wind velocity for various weight concentrations of RASH-treated samples.

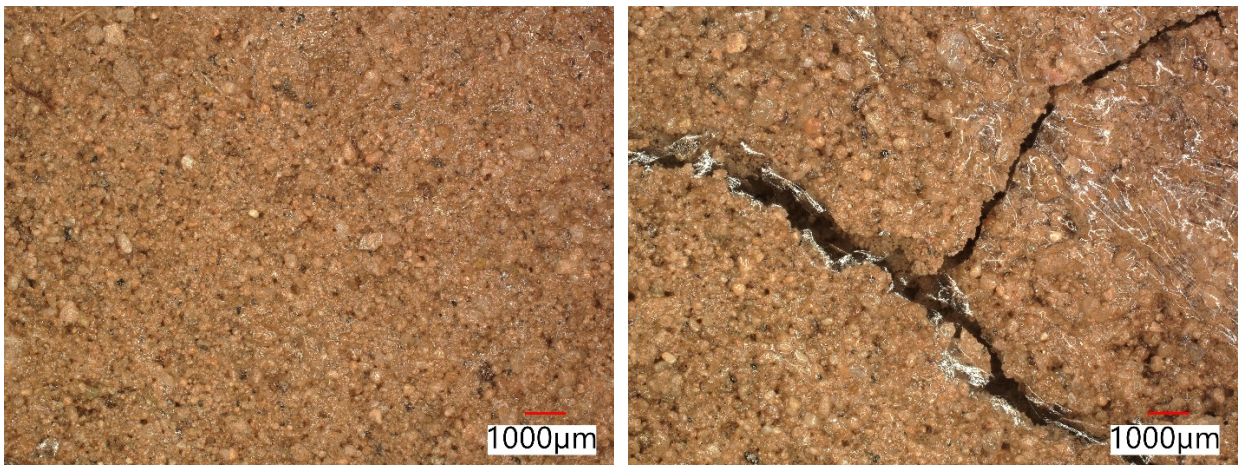

(a) (b)

Figure 3-5. Surface morphology comparison of RASH-treated soils post treatment (a) 1% wt. RASH, (b) 3% wt. RASH.

Figure 3-6 shows the appearance of treated in-lab samples after the PI-SWERL test. There is no discernible difference in the surface between the pre- and post-test RASH-treated pans, indicating effective dust suppression. The RASH-treated specimens formed a soil crust that effectively bound fine soil particles together. In contrast, the salt-treated and water-treated surfaces showed considerable particle detachment. Despite its hygroscopic nature, salt is inefficient as a dust suppressant in arid climates. It forms a crust that quickly evaporates and is prone to breaking under high wind conditions.

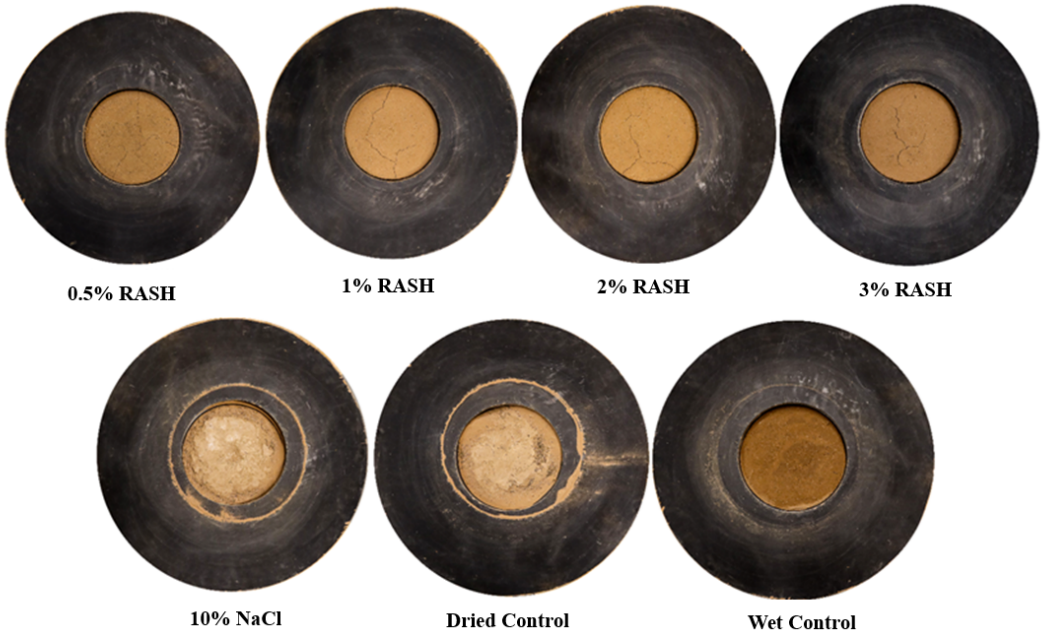

Figure 3-6. Appearance of treated surface following the PI-SWERL test.

3.2 Crust Strength Measurement

Crust strength is crucial for resisting wind erosion, especially in arid and semi-arid regions where soil is susceptible to wind erosion. To evaluate the strength of soil crust, several methods have been developed, including vane shear tests [74], cone penetration tests (CPT) [75], and flat-nose penetration tests [76]. The vane shear test measures the in-situ shear strength of soils, offering insights into their resistance to deformation. In contrast, the cone penetration test (CPT) assesses subsurface resistance by profiling soil properties at different depths. The flat-nose penetration test, however, directly quantifies the surface strength of the soil crust.

Given the significance of crust strength in mitigating wind erosion, the flat-nose penetration test is the most suitable method for this study. Note that the flat-nose penetrometer is superior to the needle penetrometer, as it distributes the load over a larger surface area, impacting multiple soil grains, whereas the needle penetrometer applies the load to only a few grains, potentially resulting in less reliable measurements of crust strength [77]. The flat-nose penetration test utilizes a 6.4 mm diameter flat-nose cylindrical probe attached to the loading piston of a universal testing machine (see Figure 3-7). The probe penetrates the specimen at a constant rate of 1.3 mm/min, measuring the normal force exerted on the crust and the resulting vertical deformation. Different concentrations of RASH, ranging from 0.5% to 3% by weight, were used and compared with the water-treated control sample. The crust strength tests were conducted 48 hours post-application, with each concentration undergoing three trials to ensure representative results.

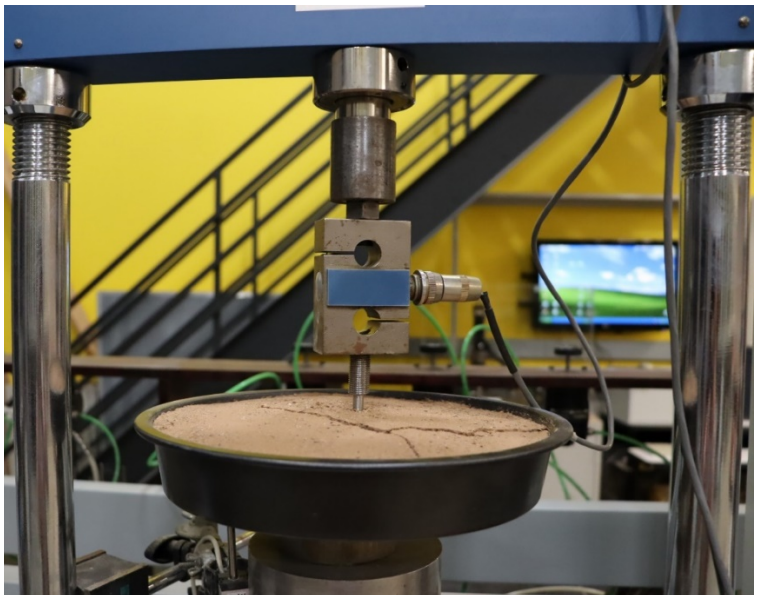

Figure 3-7. Flat-nose penetration test setup for evaluating surface crust strength.

Figure 3-8 shows the results of the penetration test for RASH-treated surfaces compared with a water-treated sample. The peak penetration resistance force of the water-treated sample was measured at 1.63 N, while RASH-treated samples demonstrated significantly higher peak penetration resistance values of 4.81 N for 0.5%wt. RASH, 6.58 N for 1%wt. RASH, 13.24 N for 2%wt. RASH, and 17.38 N for 3%wt. RASH concentrations. This substantial improvement in penetration resistance can be attributed to the formation of the crust created by the regenerated hydrogel, which binds the soil particles together and functions as an effective dust suppressant in wind-prone regions.

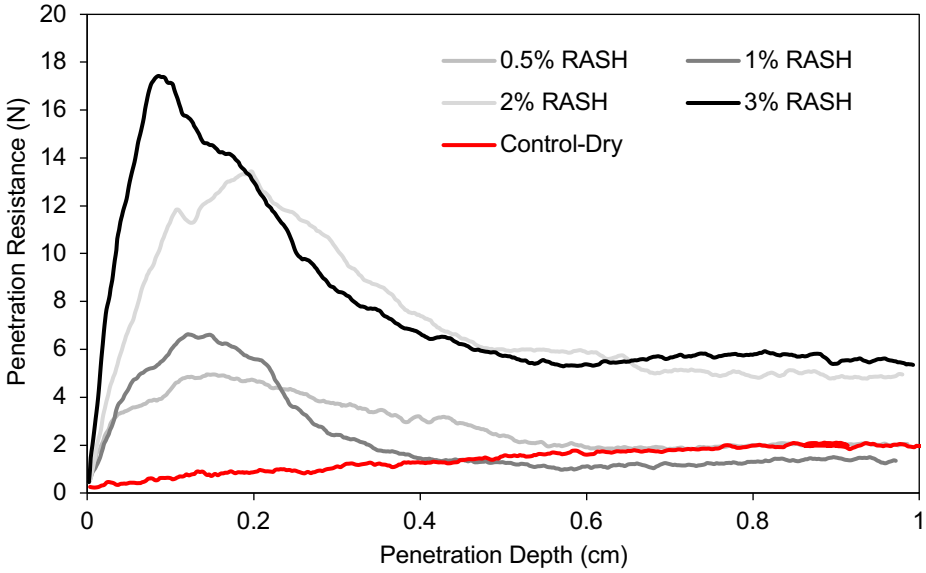

Figure 3-8. Surface penetration resistance of RASH -treated samples.

Following the penetration tests, test specimens were collected to characterize the thickness of the soil crust. This was accomplished by scraping the surface layer of specimens and extracting intact pieces of soil crust from the uppermost layer [66]. The dimensions of these intact crust samples were measured using calipers to ensure precision. The average crust thickness was derived from three trial samples, with five measurements taken at different locations on each sample, and the results are presented in Table 3-1. Notably, the 1% wt. RASH-treated samples exhibited the greatest crust thickness, striking a balance between effective penetration and medium viscosity, while providing adequate structural integrity. Conversely, the increase in viscosity observed with the 3% wt. RASH treatment resulted in a decrease in crust thickness, suggesting an inability to penetrate deeper layers and adequately fill the finer pores. In contrast, the NaCl-treated samples exhibited the formation of a brittle crust layer, indicating a lower level of stability. This fragility underscores the importance of carefully considering treatment composition to achieve ideal soil crust formation. Figure 3-9 visually compares the crust thickness between NaCl-treated and RASH-treated dust samples. The RASH-treated samples developed a significantly more robust thicker crust, highlighting their sustainable stability and effectiveness.

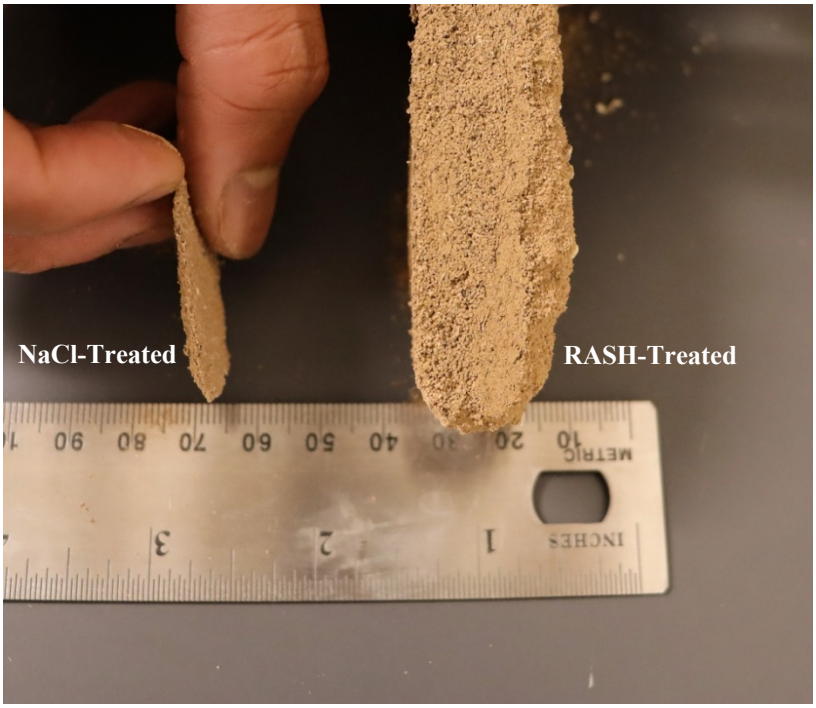

Figure 3-9. Appearance of crust thickness of 1%wt. RASH-treated surface and 10%wt. NaCl-treated surface.

Table 3-1. Crust thickness measurements based on three trial samples, with five measurement points per sample, for RASH-treated and NaCl-treated surfaces

	10%wt. NaCl	0.5%wt. RASH	1%wt. RASH	2%wt. RASH	3%wt. RASH
Crust thickness (mm)	1.71	16.12	17.11	17.03	16.85
Standard error of the mean (SEM)	0.02	0.11	0.10	0.08	0.03

3.3 Conclusion

This chapter investigated the in-lab wind erosion resistance and crust strength of soil treated with regenerated starch hydrogel (RASH). The main conclusions are summarized below:

1. RASH-treated samples at 1% and 2% wt. achieved threshold detachment wind velocities above 90 km/h, demonstrating superior dust suppression compared to water- and salt-treated controls.
2. Further inspection showed no visible surface degradation in RASH-treated samples, while water- and salt-treated soils exhibited clear particle detachment and crust failure.
3. Crust strength increased with RASH concentration, with penetration resistance rising from 4.81 N (0.5% wt.) to 17.38 N (3% wt.), compared to only 1.63 N for the water-treated control.
4. Crust thickness was greatest in 1% wt. RASH-treated soils (17.11 mm), suggesting a balance between penetration depth and viscosity. However, higher concentrations (e.g., 3% wt.) led to localized cracking due to higher viscosity.
5. Salt-treated surfaces formed brittle, thin crusts (approximately 1.71 mm) that were less effective in resisting wind erosion, highlighting the limitations of salt-based dust control under dry conditions.

Chapter 4. Performance of Regenerated Amylopectin Starch Hydrogel in Field Conditions

To scale up the application of the hydrogels as a dust mitigation technique, a comprehensive field trial was conducted at a construction site in Tempe, Arizona. The efficiency of various treatments, including 1% wt. RASH and 10% wt. NaCl, was compared to a control group treated with water. The 1% wt. RASH concentration was chosen as the ideal concentration based on lab results (see previous section). Wind erosion resistance was assessed using the PI-SWERL device at the end of 2, 5, 10, and 20 days post-application. This study was performed on two distinct soil types, fine sand (Site A) and well-graded sand with gravel (Site B), to capture the variability in dust generation potential across typical construction environments. Treatments were applied under the hot and dry conditions of the Arizona summer to evaluate long-term performance under realistic climatic stress. PM10 concentration data collected from PI-SWERL testing served as the primary metric for dust emission.

4.1 Field Site Characteristics

The field trial was conducted at an inactive construction site in Tempe, Arizona, as illustrated in Figure 4-1. This site comprises two distinct soil covers: one predominantly composed of fine sand (Site A) and the other characterized by gravel (Site B). Soil samples were collected from designated treatment plots at both sites, and particle size distribution analysis was then performed using standard sieve analysis methods.

Figure 4-1.a) Location of the construction site, b) ground-level view of the site.

The particle size distribution of the soil is presented in Figure 4-2. According to the Unified Soil Classification System (USCS)[67], Site A has well-graded sand, while Site B has well-graded sand with gravel. Detailed results of the sieve analysis are summarized in Table 4-1, and the visual characteristics of soil at each site are shown in Figure 4-3. Site A, dominated by fine sand, presents a higher potential for dust generation, making it an ideal candidate for testing dust mitigation strategies. Conversely, Site B, with its well-graded sand with gravel, serves as a better

representative of an unpaved area, providing insights into the performance of the RASH treatment on gravel roads.

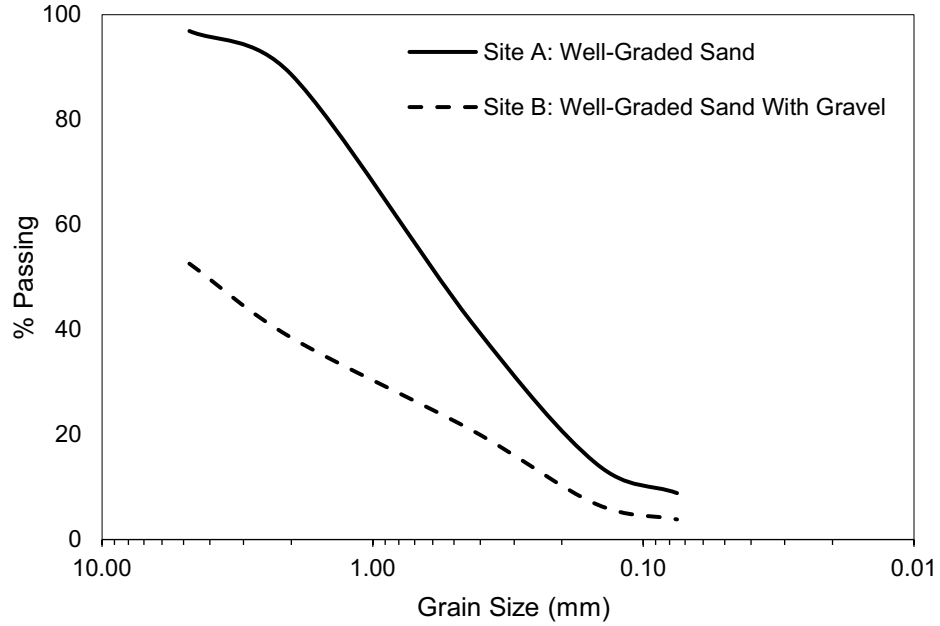

Figure 4-2. Particle size distribution of construction site

Table 4-1.Results of sieve analysis for the construction sites

	Gravel (%)	Sand (%)	Fines (%)	D_{50}(mm)	Coefficient of Uniformity (C_u)	Coefficient of Curvature (C_c)
Site A	47.44	48.70	3.86	4.25	22.27	1.53
Site B	3.10	88.04	8.86	0.72	11.66	1.03

(a) (b)

Figure 4-3. Appearance of the soil in (a) construction Site A with well-graded sand, and (b) construction Site B with well-graded sand with gravel.

4.2 Plot treatment

Three test plots were established at each construction site, including those treated with 1%wt. RASH, 10%wt. NaCl, and a control group treated with water. Figure 4-4 depicts the layout configuration of these three test plots. Each plot comprises three squares, each with a side length of 25 inches, and a spacing of 25 inches between squares to facilitate sampling and visual observations.

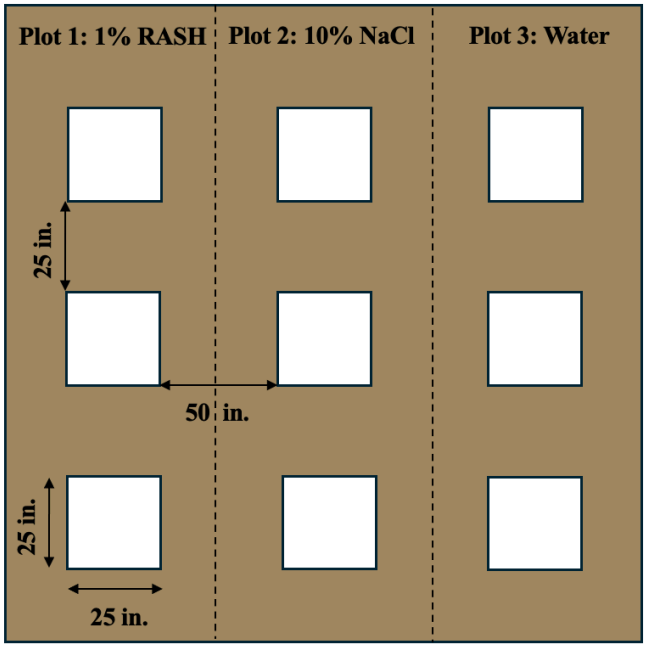

Figure 4-4. Configuration of test plots layout for each construction site.

The dust suppressants were applied to each plot using a pump sprayer at a consistent application rate of 2.5 liters/m² , as recommended by Wooley [66] for adequate coverage in similar applications. Field dust measurements were performed with the PI-SWERL 2-, 5-, 10-, and, 20-days post-application to evaluate the treatments over a longer period when compared to in-lab tests. It is noteworthy that the applications occurred during the daytime heat of June and July in Arizona's arid climate, with an average daily temperatures around 39°C and relative humidity approximately 23% throughout the 20-day evaluation period. Figure 4-5 illustrates the dust measurements recorded at Site A using the PI-SWERL device 48 hours after treatment.

Figure 4-5. View of the field trial area after treatment.

4.3 Site A: dust measurements

Site A, dominated by fine sand, exhibited a prominent crust on the ground surface across all treated test plots. Figure 4-6.a shows the PM10 concentration results at various wind velocities, recorded 48 hours after the application of the dust suppressants. The water-treated surface was dried prior to testing, and substantial particle detachment was observed when wind velocities surpassed 57.6 km/h. To better compare the efficiency of each product, Figure 4-6.b compares the dust measurements for different dust suppressants, excluding water as the control group.

Surfaces treated with 1%wt. RASH and 10%wt. NaCl exhibited substantial resilience, effectively withstanding the maximum safe wind speeds of the PI-SWERL test. The hygroscopic properties of the 10%wt. NaCl solution facilitate moisture retention, thereby reducing dust emissions, while the 1%wt. RASH forms a robust crust on the surface by agglomerating soil particles; the strong forces generated by inter-particle bonding between soil grains and regenerated hydrogel enhance soil surface cohesion and reduce vulnerability to erosion and dust generation.

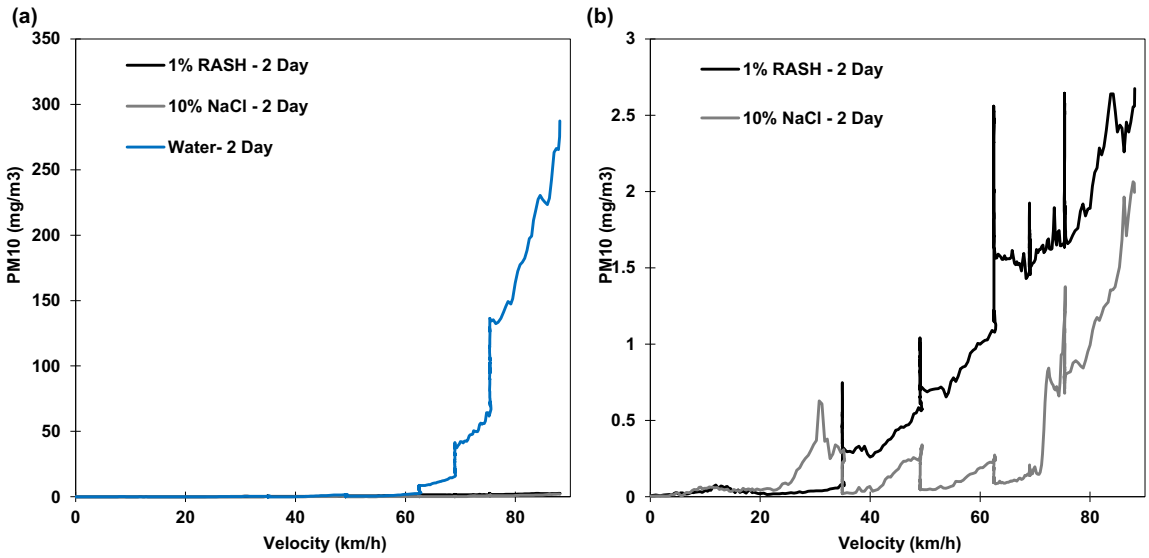

Figure 4-6. Particulate matter (PM10) concentration as a function of velocity in the PI-SWERL test at construction Site A, 48 hours post-treatment: (a) comparison between water treatment and other dust suppressants, (b) comparison between effective dust suppressants

Figure 4-7 shows the appearance of the treated surfaces 48 hours after treatment. No significant detachment is observed in RASH-treated case after the PI-SWERL test, indicating the general dust suppression efficiency. The presence of some dust in Figure 4-7 .a is due to particles adhering to the rubber collar of the PI-SWERL device, rather than indicating detachment from the surface. Additionally, the white precipitate observed on the soil surface in the 10% NaCl-treated plot is due to the salt's presence, which aids in moisture retention.

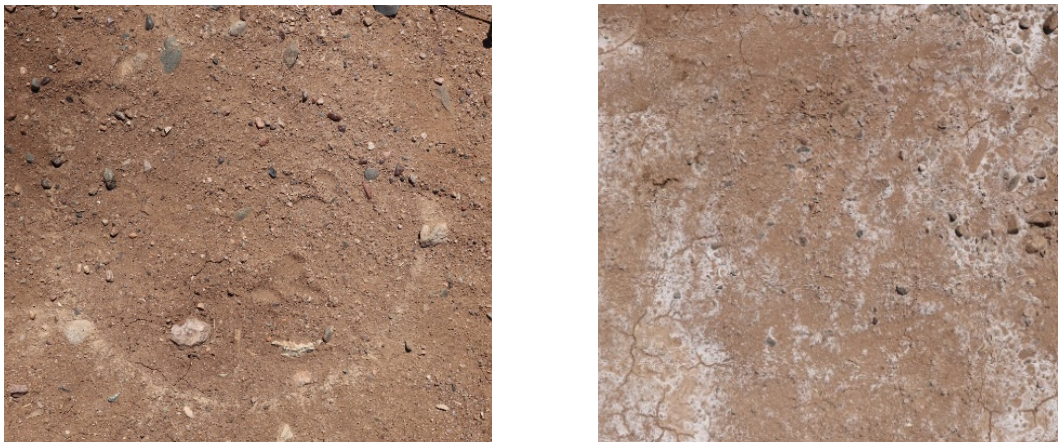

(a) (b)

Figure 4-7. Appearance of field treated surfaces 48 hours post-treatment: (a) 1%wt. *RASH*, (b) 10%wt. NaCl.

To evaluate the long-term performance of each dust suppressant, PM10 measurements were conducted after 5, 10, and 20 days following the application of the treatments to the soil

surface. Figure 4-8 illustrates the results for the 1%wt. RASH and 10%wt. NaCl treatments. This study reveals that the maximum detectable PM10 concentration after 20 days remains as low as 12 mg/m³ for both treatments. This low concentration underscores the long-term efficacy of these dust suppressants, even under the severe, arid conditions and intense UV exposure prevalent in Arizona.

For the 10% NaCl treatment, the salt not only retains moisture in the soil but also penetrates into the pores, filling spaces and cracks. The sustained low PM10 levels with 1%wt. RASH can be attributed to the strong inter-particle bonding provided by regenerated hydrogel, which enhances soil cohesion. In addition to its strong performance, RASH is a biodegradable and non-corrosive material, making it a more sustainable alternative to conventional salt-based suppressants. Moreover, it does not become an additional source of dust like salt at low relative humidity conditions.

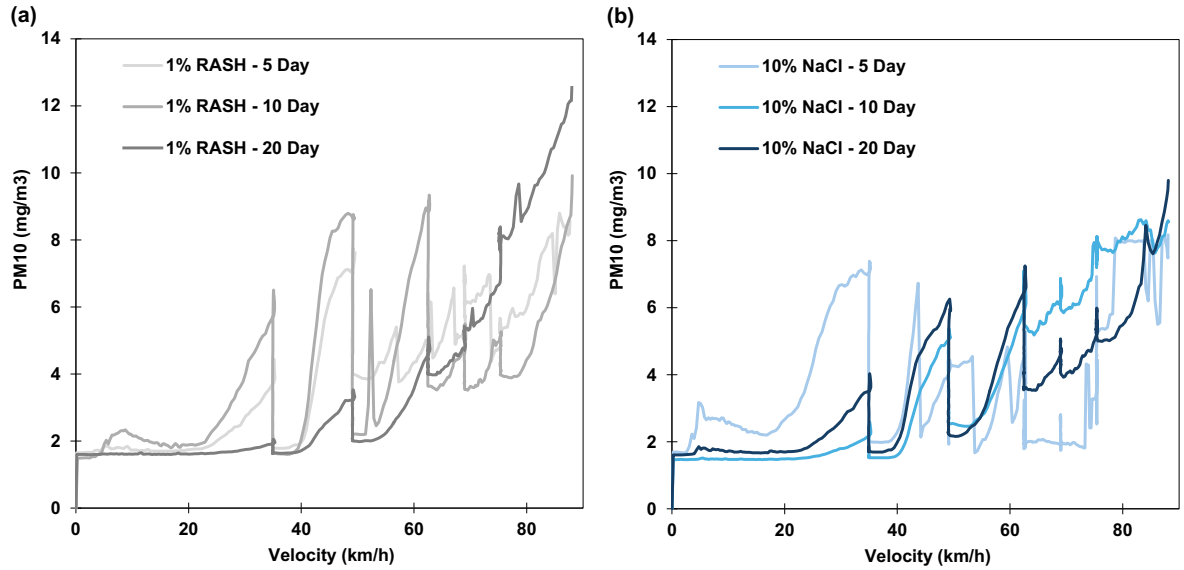

Figure 4-8. Particulate matter (PM10) concentration as a function of velocity at construction site A at different time intervals (5 days, 10 days, and 20 days) post-application: (a) 1% wt. RASH, (b) 10%wt. NaCl.

4.4 Site B: dust measurements

Construction Site B, characterized by its composition of well-graded sand and gravel, serves as a representative of gravel roads. Figure 4-9 presents the PM10 concentration results at different wind velocities 48 hours after the application of dust suppressants. The surface treated with water completely evaporated, with significant particle detachment observed at wind velocities exceeding 64.8 km/h. Figure 4-9.b provides a comparative analysis of the dust suppressants, excluding water as the control group.

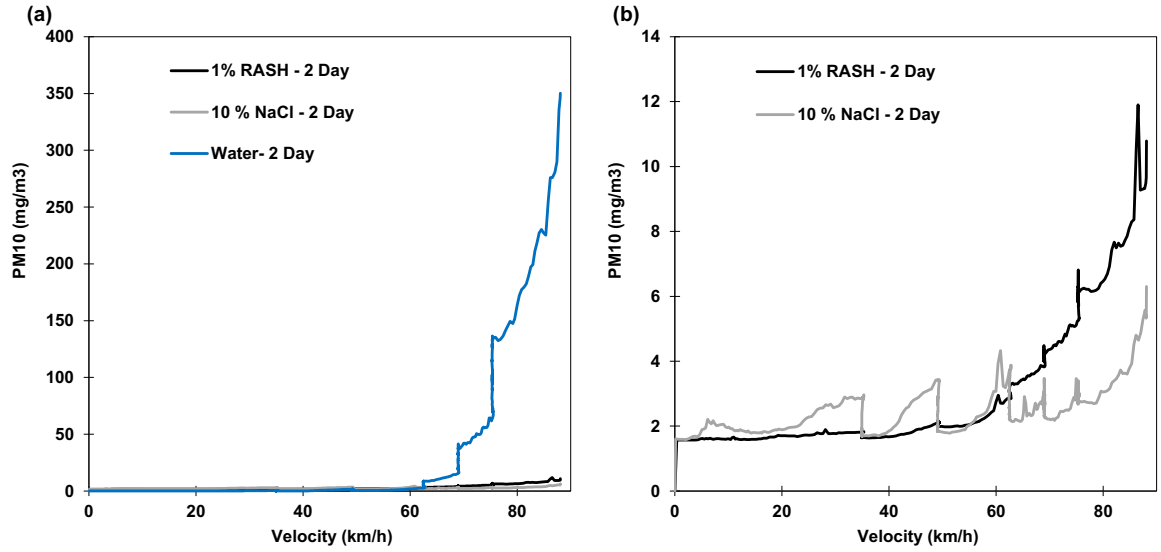

Figure 4-9. PM10 concentration versus velocity in PI-SWERL test at construction Site B, 48 hours after treatment: (a) comparison of water treatment with other dust suppressants, (b) comparison of effective dust suppressants.

Figure 4-10 shows the appearance of the treated surfaces 48 hours after treatment. Some detachment is observed in both plots treated with 1%wt. RASH and 10%wt. NaCl due to the varying size of the grains.

(a) (b)

Figure 4-10. Appearance of field treated surfaces 48 hours post-treatment at construction Site B: (a) treated with 1%wt. RASH, (b) treated with 10%wt. NaCl.

Similar to Construction Site A, long-term efficiency of each dust suppressant was evaluated 5-, 10-, and 20-days post-application. Figure 4-11 presents results of these measurements for 1%wt. RASH and 10%wt. NaCl treatments. After 20 days, the maximum detectable PM10 concentration was approximately 40 mg/m³ for 1%wt. RASH and 90 mg/m³ for 10% NaCl. Notably, 1%wt. RASH treatment demonstrated significantly greater effectiveness in mitigating

dust compared to the 10%wt. NaCl. This can be attributed to the hydrogel's enhanced capacity to form a stable crust through stronger inter-particle bonding. Unlike construction Site A, 10%wt. NaCl is less effective because its hygroscopic nature alone is insufficient to suppress the dust, as Site B has larger particles that have to be agglomerated for better dust suppression efficiency.

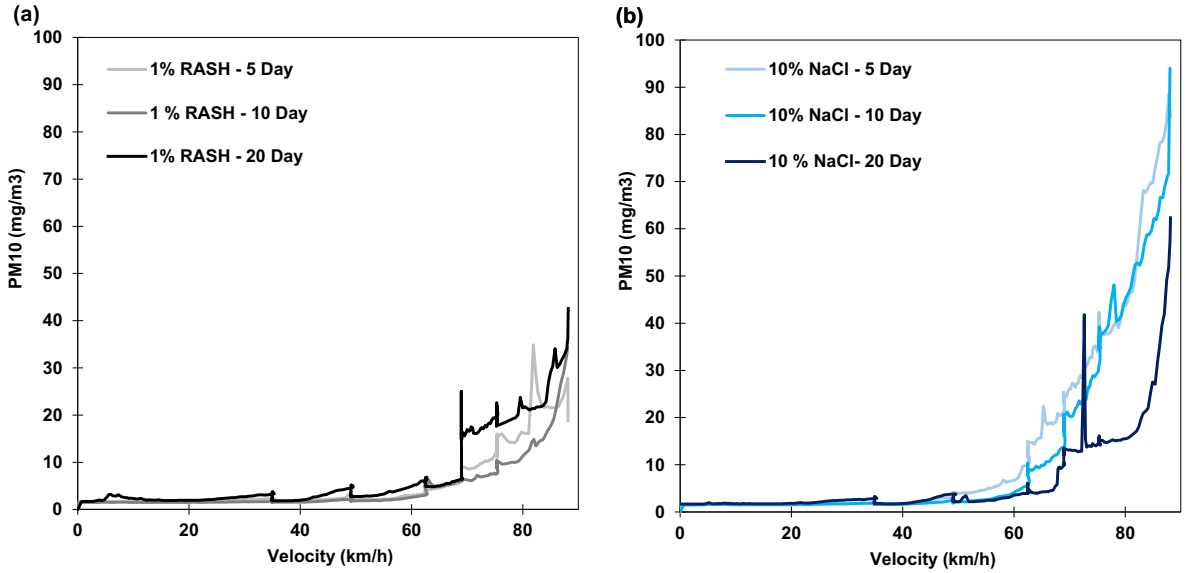

Figure 4-11. Particulate matter (PM10) concentration as a function of velocity at construction Site B at different time intervals (2 Days, 5 Days, 10 Days, and 20 days) post-application: (a) 1%wt. RASH, (b) 10%wt. NaCl.

4.5 Conclusion

This chapter evaluated the field performance of regenerated starch hydrogel (RASH) in comparison to salt and water treatments under typical construction site conditions. The key findings are summarized below:

1. At Site A (fine sand), both 1% wt. RASH and 10% wt. NaCl significantly reduced PM10 emissions, with maximum detectable concentrations remaining below 12 mg/m³ after 20 days, confirming strong long-term dust suppression under arid conditions.
2. At Site B (well-graded sand with gravel), 1% wt. RASH outperformed 10% wt. NaCl, achieving lower PM10 levels (~40 mg/m³ vs. 90 mg/m³ after 20 days), demonstrating that hydrogel treatment was more effective for coarse, less cohesive soils.
3. RASH-treated plots maintained visible surface integrity and showed minimal particle detachment even after 20 days of exposure to heat and wind, while salt-treated surfaces exhibited visible white precipitates and were less stable on coarser soils.
4. Unlike salt, RASH does not contribute to surface salinity, dust regeneration, or soil degradation, making it a more environmentally sustainable and non-corrosive alternative for dust suppression.
5. These results validate the field applicability of RASH as a reliable and biodegradable solution for dust control across varying soil textures and environmental conditions.

Chapter 5. Conclusions and Recommendations

This study proposed a regenerated amylopectin starch hydrogel (RASH) as a sustainable, shelf-stable dust suppressant for mitigating particulate emissions in arid environments. Laboratory and field experiments were conducted to evaluate its effectiveness compared to conventional salt-based and water-based dust control treatments. The study focused on understanding the wind erosion resistance, surface crust formation, and long-term stability of RASH-treated soils under both controlled and natural conditions.

5.1 Conclusions

1. The regenerated starch hydrogel developed in this study was synthesized in powder form, making it shelf-stable, easily transportable, and suitable for on-demand field applications without the need for synthetic additives or cold storage. Its simplicity and adaptability make it a practical solution for dust suppression in remote or resource-limited settings.
2. Laboratory wind erosion tests demonstrated that RASH-treated samples at 1% and 2% weight concentrations achieved complete resistance to wind speeds up to 90 km/h. The 1% wt. dosage provided the balance of soil infiltration, crust strength, and application ease. In contrast, 3% wt. concentration led to excessive viscosity, restricting penetration and resulting in surface cracking and localized shrinkage.
3. Compared to salt-based treatments, RASH showed significantly better performance under dry conditions. While 10% wt. NaCl-treated surfaces exhibited particle detachment at relatively low wind velocities, RASH maintained strong inter-particle bonding and surface integrity even after 48 hours of drying, highlighting its effectiveness when moisture availability is limited.
4. Field tests at a construction site in Tempe, Arizona, validated RASH's long-term dust suppression capability. On fine sandy soils, RASH reduced PM_{10} emissions to below 2.5 mg/m^3 and sustained this reduction for up to 20 days despite exposure to high temperatures, low humidity, and intense UV radiation. On gravel-based soils, RASH also performed better than salt, demonstrating versatility across soil textures.
5. In addition to strong technical performance, RASH offers an environmentally sustainable alternative to conventional dust suppressants. It is biodegradable, non-corrosive, and does not contribute to soil salinization or secondary dust emissions, making it suitable for long-term application in sensitive environments.

5.2 Recommendations for Future Work

Future research should evaluate the performance of RASH across a wider range of soil types and environmental conditions to confirm its generalizability. Studies should also investigate its durability under repeated wetting and drying cycles, temperature fluctuations, and long-term UV exposure. It is recommended that a full life cycle assessment (LCA) be conducted to quantify the environmental impact of RASH production, application, and degradation. In parallel, further

optimization of the hydrogel formulation, including starch source, particle size, and regeneration technique, should be explored to improve absorption behavior and crust durability. Finally, the integration of RASH with other bio-based or mineral additives could be examined to enhance its performance in extreme climates or broaden its functionality for erosion control, slope stabilization, or other geotechnical applications.

References

[1] Ambient (outdoor) air pollution, (n.d.). https://www.who.int/news-room/fact-sheets/detail/ambient-(outdoor)-air-quality-and-health (accessed November 2, 2024).

[2] I. Manisalidis, E. Stavropoulou, A. Stavropoulos, E. Bezirtzoglou, Environmental and health impacts of air pollution: a review, Frontiers in Public Health 8 (2020) 14.

[3] C.-H. Lee, L.-W. Tang, C.T. Chang, Modeling of Fugitive Dust Emission for Construction Sand and Gravel Processing Plant, Environ. Sci. Technol. 35 (2001) 2073–2077. https://doi.org/10.1021/es001237y.

[4] H. Noh, S. Lee, J. Yu, Identifying effective fugitive dust control measures for construction projects in Korea, Sustainability 10 (2018) 1206.

[5] F.S. Pianalto, S.R. Yool, Monitoring fugitive dust emission sources arising from construction: a remote-sensing approach, GIScience & Remote Sensing 50 (2013) 251–270. https://doi.org/10.1080/15481603.2013.808517.

[6] Y. Liu, L. Shao, W. Wang, J. Chen, H. Zhang, Y. Yang, B. Hu, Study on fugitive dust control technologies of agricultural harvesting machinery, Agriculture 12 (2022) 1038.

[7] K. Saxton, D. Chandler, L. Stetler, B. Lamb, C. Claiborn, B.-H. Lee, Wind erosion and fugitive dust fluxes on agricultural lands in the Pacific Northwest, Transactions of the ASAE 43 (2000) 623–640.

[8] B. Chakradhar, Fugitive dust emissions from mining areas, Journal of Environmental Systems 31 (2005). https://access.portico.org/Portico/show?viewFile=pdf&auId=pgk5sxhmhq (accessed November 2, 2024).

[9] M.M. Kahraman, M. Erkayaoglu, A Data-Driven Approach to Control Fugitive Dust in Mine Operations, Mining, Metallurgy & Exploration 38 (2021) 549–558. https://doi.org/10.1007/s42461-020-00318-2.

[10] D. Barnes, B. Connor, Managing dust on unpaved roads and airports, Alaska University Transportation Center, 2014. https://scholarworks.alaska.edu/handle/11122/8813 (accessed November 2, 2024).

[11] R.I.J. Dyck, J.J. Stukel, Fugitive dust emissions from trucks on unpaved roads, Environ. Sci. Technol. 10 (1976) 1046–1048. https://doi.org/10.1021/es60121a015.

[12] J.A. Organiscak, W.M. Randolph Reed, Characteristics of Fugitive Dust Generated from Unpaved Mine Haulage Roads, International Journal of Surface Mining, Reclamation and Environment 18 (2004) 236–252. https://doi.org/10.1080/1389526042000263333.

[13] S. Parvej, D.L. Naik, H.U. Sajid, R. Kiran, Y. Huang, N. Thanki, Fugitive dust suppression in unpaved roads: State of the art research review, Sustainability 13 (2021) 2399.

[14] G. Zhao, Y. Chen, P.K. Hopke, T.M. Holsen, S. Dhaniyala, Characteristics of traffic-induced fugitive dust from unpaved roads, Aerosol Science and Technology 51 (2017) 1324–1331. https://doi.org/10.1080/02786826.2017.1347251.

[15] M. Ansarinejad, Y. Huang, A. Qiu, Impact of Fog on Vehicular Emissions and Fuel Consumption in a Mixed Traffic Flow with Autonomous Vehicles (AVs) and Human-Driven Vehicles Using VISSIM Microsimulation Model, in: International Conference on Transportation and Development 2023, American Society of Civil Engineers, Austin, Texas, 2023: pp. 253–262. https://doi.org/10.1061/9780784484876.023.

[16] C. Vahlsing, K.R. Smith, Global review of national ambient air quality standards for PM10 and SO2 (24 h), Air Qual Atmos Health 5 (2012) 393–399. https://doi.org/10.1007/s11869-010-0131-2.

[17] M.A. Barrero, J.A.G. Orza, M. Cabello, L. Cantón, Categorisation of air quality monitoring stations by evaluation of PM10 variability, Science of The Total Environment 524 (2015) 225–236.

[18] K.-H. Kim, Z.-H. Shon, Long-term changes in PM10 levels in urban air in relation with air quality control efforts, Atmospheric Environment 45 (2011) 3309–3317.

[19] Fugitive Dust Control Measures and Best Practices, (n.d.).

[20] H. Jin, W. Nie, Y. Zhang, H. Wang, H. Zhang, Q. Bao, J. Yan, Development of Environmental Friendly Dust Suppressant Based on the Modification of Soybean Protein Isolate, Processes 7 (2019) 165. https://doi.org/10.3390/pr7030165.

[21] Y. Hu, L. Shi, Z. Shan, R. Dai, H. Chen, Efficient removal of atmospheric dust by a suppressant made of potato starch, polyacrylic acid and gelatin, Environ Chem Lett 18 (2020) 1701–1711. https://doi.org/10.1007/s10311-020-01025-6.

[22] S.W. Morefield, J.K. Newman, C.A. Weiss Jr, C.C. Thomas, P.G. Malone, Corrosion Inhibitive Hygroscopic Organic-Based Dust Palliatives, (2018). https://apps.dtic.mil/sti/trecms/pdf/AD1081140.pdf (accessed November 2, 2024).

[23] Y. Xi, Z. Xie, Corrosion effects of magnesium chloride and sodium chloride on automobile components, Colorado Department of Transportation, Research [Branch], 2002. https://www.codot.gov/programs/research/reports/2002/magautocor.pdf (accessed November 2, 2024).

[24] K. Edvardsson, Gravel Roads and Dust Suppression, Road Materials and Pavement Design 10 (2009) 439–469. https://doi.org/10.1080/14680629.2009.9690209.

[25] C.-M. Geilfus, Chloride in soil: From nutrient to soil pollutant, Environmental and Experimental Botany 157 (2019) 299–309.

[26] D.Q. Tong, T.E. Gill, W.A. Sprigg, R.S. Van Pelt, A.A. Baklanov, B.M. Barker, J.E. Bell, J. Castillo, S. Gassó, C.J. Gaston, D.W. Griffin, N. Huneeus, R.A. Kahn, A.P. Kuciauskas, L.A.

Ladino, J. Li, O.L. Mayol-Bracero, O.Z. McCotter, P.A. Méndez-Lázaro, P. Mudu, S. Nickovic, D. Oyarzun, J. Prospero, G.B. Raga, A.U. Raysoni, L. Ren, N. Sarafoglou, A. Sealy, Z. Sun, A.V. Vimic, Health and Safety Effects of Airborne Soil Dust in the Americas and Beyond, Reviews of Geophysics 61 (2023) e2021RG000763. https://doi.org/10.1029/2021RG000763.

[27] B.K. Kunz, E.E. Little, V.L. Barandino, Aquatic Toxicity of Chemical Road Dust Suppressants to Freshwater Organisms, Arch Environ Contam Toxicol 82 (2022) 294–305. https://doi.org/10.1007/s00244-020-00806-y.

[28] B.A. Goodrich, R.D. Koski, W.R. Jacobi, Monitoring Surface Water Chemistry Near Magnesium Chloride Dust Suppressant Treated Roads in Colorado, J of Env Quality 38 (2009) 2373–2381. https://doi.org/10.2134/jeq2009.0042.

[29] T. Tonu, Environmentally friendly alternatives to reduce dust emission and salt use in the sand and stone production industry, Master's Thesis, T. Tonu, 2023. https://oulurepo.oulu.fi/handle/10024/42341 (accessed November 2, 2024).

[30] A.S. Kolawole, A.O. Iyiola, Environmental Pollution: Threats, Impact on Biodiversity, and Protection Strategies, in: S.C. Izah, M.C. Ogwu (Eds.), Sustainable Utilization and Conservation of Africa's Biological Resources and Environment, Springer Nature Singapore, Singapore, 2023: pp. 377–409. https://doi.org/10.1007/978-981-19-6974-4_14.

[31] A. Almajed, K. Lemboye, M.G. Arab, A. Alnuaim, Mitigating wind erosion of sand using biopolymer-assisted EICP technique, Soils and Foundations 60 (2020) 356–371.

[32] X.U.E. Zhenglong, W. Guanhua, S.U.N. Hao, Z. Yunli, S.I. Chuanling, J.I.A. Hongyu, Research Status and Development Trend of Bio-based Dust Suppressants., Biomass Chemical Engineering 57 (2023). https://search.ebscohost.com/login.aspx?direct=true&profile=ehost&scope=site&authtype=crawler&jrnl=16735854&AN=163122535&h=d5RbQMeS8hIFV6S%2BExKofIy%2BZiZeyROty4Co3kMbZYYgsHMTaJ2ApS2wWXmkuSJT4o5TUXh0mp%2B1RaHdZOyB0Q%3D%3D&crl=c (accessed November 2, 2024).

[33] J.L. Sieger, B.G. Lottermoser, J. Freer, Effectiveness of Protein and Polysaccharide Biopolymers as Dust Suppressants on Mine Soils: Large-Scale Field Trials, Mining 3 (2023) 428–462.

[34] R. Wang, H. Yu, Y. Xie, W. Li, H. Qi, Study on protein-polysaccharide environmental foam dust suppressant based on Maillard reaction, Journal of Molecular Liquids 410 (2024) 125644.

[35] Y. Zhu, Y. Cui, Z. Shan, R. Dai, L. Shi, H. Chen, Fabrication and characterization of a multi-functional and environmentally-friendly starch/organo-bentonite composite liquid dust suppressant, Powder Technology 391 (2021) 532–543. https://doi.org/10.1016/j.powtec.2021.06.050.

[36] X. Dang, Z. Shan, H. Chen, Usability of oxidized corn starch–gelatin blends for suppression and prevention of dust, J of Applied Polymer Sci 134 (2017) app.44437. https://doi.org/10.1002/app.44437.

[37] R. Xu, H. Yu, H. Dong, Y. Ye, S. Xie, Preparation and properties of modified starch-based low viscosity and high consolidation foam dust suppressant, Journal of Hazardous Materials 452 (2023) 131238.

[38] S. Khadse, K. Sekhar, G. Begum, B.H. Rao, Effectiveness of Xanthan Gum and Guar Gum in Mitigating Dust Emission from Bauxite Residue Tailings Facility, Indian Geotech J (2024). https://doi.org/10.1007/s40098-024-01051-z.

[39] X. Wang, H. Chen, Y. Shi, Y. Lin, J. Yang, X. Li, Development of an eco-friendly dust suppressant based on modified guar gum: Performance and mechanism analysis, Powder Technology 439 (2024) 119681.

[40] H. Zhang, W. Nie, H. Wang, Q. Bao, H. Jin, Y. Liu, Preparation and experimental dust suppression performance characterization of a novel guar gum-modification-based environmentally-friendly degradable dust suppressant, Powder Technology 339 (2018) 314–325.

[41] M. Liu, Q. Meng, C. Niu, Y. Wang, G. Zhou, C. Xu, Y. Liu, Preparation and characterization of modified dual network dust suppression gel based on sodium alginate and soluble starch, Environ Sci Pollut Res 29 (2022) 69771–69784. https://doi.org/10.1007/s11356-022-20721-0.

[42] Y. Liu, C. Du, F. Yi, C. Cheng, M. Wang, Modified sodium alginate-based three-dimensional network hydrogel dust suppressant: Preparation, characterization, and performance, International Journal of Biological Macromolecules 274 (2024) 133408.

[43] W. Nie, W. Niu, Q. Bao, M. Yuan, W. Zhou, Y. Hua, F. Yu, C. Liu, S. Zhang, X. Zhang, Study on the combined dust suppression effect of sodium alginate and sodium fatty acid methyl ester sulfonate, Advanced Powder Technology 33 (2022) 103827.

[44] H. Wang, W. Nie, H. Zhang, H. Jin, Q. Bao, J. Yan, Q. Liu, A Synthesis of a Dust Suppressant Using the Cellulose Extracted from Maize Straw, Starch StäRke 72 (2020) 1900187. https://doi.org/10.1002/star.201900187.

[45] Y. Yang, Q. Zhao, Y. Mi, Preparation and Optimum Proposal of Biological Dust Suppressant Using Straw Based on Orthogonal Test, J. Highway Transp. Res. Dev. (English Ed.) 15 (2021) 8–17. https://doi.org/10.1061/JHTRCQ.0000771.

[46] Y. Liu, W. Nie, H. Jin, H. Ma, Y. Hua, P. Cai, W. Wei, Solidifying dust suppressant based on modified chitosan and experimental study on its dust suppression performance, Adsorption Science & Technology 36 (2018) 640–654. https://doi.org/10.1177/0263617417713624.

[47] G. Zhou, Z. Xing, Y. Tian, B. Jiang, B. Ren, X. Dong, L. Yi, An environmental-friendly oil-based dust suppression microcapsules: Structure with chitosan derivative as capsule wall, Process Safety and Environmental Protection 165 (2022) 453–462.

[48] C. Li, Recent progress in understanding starch gelatinization - An important property determining food quality, Carbohydrate Polymers 293 (2022) 119735. https://doi.org/10.1016/j.carbpol.2022.119735.

[49] J. Sun, G. Zhou, D. Gao, Z. Wei, N. Wang, Preparation and performance characterization of a composite dust suppressant for preventing secondary dust in underground mine roadways, Chemical Engineering Research and Design 156 (2020) 195–208. https://doi.org/10.1016/j.cherd.2020.01.030.

[50] Z. Liang, X. Cai, H. Hu, Y. Zhang, Y. Chen, Z. Huang, Synthesis of starch-based super absorbent polymer with high agglomeration and wettability for applying in road dust suppression, International Journal of Biological Macromolecules 183 (2021) 982–991.

[51] (PDF) Lignin as Potent Industrial Biopolymer: An Introduction, (n.d.). https://www.researchgate.net/publication/339875116_Lignin_as_Potent_Industrial_Biopolymer_An_Introduction (accessed April 25, 2025).

[52] Lignin and Lignans as Renewable Raw Materials: Chemistry, Technology and Applications | Wiley, Wiley.Com (n.d.). https://www.wiley.com/en-be/Lignin+and+Lignans+as+Renewable+Raw+Materials%3A+Chemistry%2C+Technology+and+Applications-p-9781118597866 (accessed April 25, 2025).

[53] Solidifying dust suppressant based on modified chitosan and experimental study on its dust suppression performance - Yanghao Liu, Wen Nie, Hu Jin, He Ma, Yun Hua, Peng Cai, Wenle Wei, 2018, (n.d.). https://journals.sagepub.com/doi/full/10.1177/0263617417713624 (accessed April 25, 2025).

[54] K. Ravishankar, M. Venkatesan, R.P. Desingh, A. Mahalingam, B. Sadhasivam, R. Subramaniyam, R. Dhamodharan, Biocompatible hydrogels of chitosan-*alkali* lignin for potential wound healing applications, Materials Science and Engineering: C 102 (2019) 447–457. https://doi.org/10.1016/j.msec.2019.04.038.

[55] Y. Xu, B. Ma, Y. Zhang, Y. Fan, Optimal Preparation and Performance Study of Eco-Friendly Composite Chemical Dust Suppressants: A Case Study in a Construction Site in Chengdu, Materials 17 (2024) 2346. https://doi.org/10.3390/ma17102346.

[56] Gelatinizing Starch in Sodium Hydroxide/Glycerol Aqueous Solution at Room Temperature - Yang - 2021 - Starch - Stärke - Wiley Online Library, (n.d.). https://onlinelibrary.wiley.com/doi/abs/10.1002/star.202000152 (accessed April 25, 2025).

[57] Y. Cheng, H. Yuqing, L. Xiao, W. Gao, X. Kang, J. Sui, B. Cui, Impact of starch amylose and amylopectin on the rheological and 3D printing properties of corn starch, International

Journal of Biological Macromolecules 278 (2024) 134403. https://doi.org/10.1016/j.ijbiomac.2024.134403.

[58] M. Schirmer, M. Jekle, T. Becker, Starch gelatinization and its complexity for analysis, Starch - Stärke 67 (2015) 30–41. https://doi.org/10.1002/star.201400071.

[59] L. Zhang, J. Zhao, F. Li, X. Jiao, Y. Zhang, B. Yang, Q. Li, Insight to starch retrogradation through fine structure models: A review, International Journal of Biological Macromolecules 273 (2024) 132765. https://doi.org/10.1016/j.ijbiomac.2024.132765.

[60] M. Tagrida, S. Gulzar, O. Martín-Belloso, P. Elez-Martínez, R. Soliva-Fortuny, Ultrasound and freeze-thaw modifications of cassava starch: Microstructure, functionality, and 3D printing potential, Food Hydrocolloids 162 (2025) 110963. https://doi.org/10.1016/j.foodhyd.2024.110963.

[61] M. Obadi, Y. Qi, B. Xu, High-amylose maize starch: Structure, properties, modifications and industrial applications, Carbohydrate Polymers 299 (2023) 120185. https://doi.org/10.1016/j.carbpol.2022.120185.

[62] B. Biduski, W.M.F. da Silva, R. Colussi, S.L. de M. El Halal, L.-T. Lim, Á.R.G. Dias, E. da Rosa Zavareze, Starch hydrogels: The influence of the amylose content and gelatinization method, International Journal of Biological Macromolecules 113 (2018) 443–449.

[63] G. Xu, X. Ding, M. Kuruppu, W. Zhou, W. Biswas, Research and application of non-traditional chemical stabilizers on bauxite residue (red sand) dust control, a review, Science of The Total Environment 616–617 (2018) 1552–1565. https://doi.org/10.1016/j.scitotenv.2017.10.158.

[64] Z.Y. Zhang YunYi, W.W. Wu Wei, L.H. Liu HongBin, Factors affecting variations of soil pH in different horizons in hilly regions., (2019). https://www.cabidigitallibrary.org/doi/full/10.5555/20193343360 (accessed November 2, 2024).

[65] K.K. Patel, A.K. Shah, A.M. Latare, Effects of Hydrogel on Physical and Chemical Properties of Soil, International Journal of Plant & Soil Science 35 (2023) 129–135. https://doi.org/10.9734/ijpss/2023/v35i82889.

[66] M.A. Woolley, Laboratory and Field Evaluation of Enzyme Induced Carbonate Precipitation (EICP) for Fugitive Dust Mitigation, PhD Thesis, Arizona State University, 2023. https://search.proquest.com/openview/1c99ed100120573b790ff79836f721c3/1?pq-origsite=gscholar&cbl=18750&diss=y (accessed April 10, 2024).

[67] A.C.D.-18 on Soil, Rock, Standard practice for classification of soils for engineering purposes (unified soil classification system) 1, ASTM international, 2017.

[68] M. Dąbski, I. Badura, M. Kycko, A. Grabarczyk, R. Matlakowska, J.-C. Otto, The Development of Limestone Weathering Rind in a Proglacial Environment of the Hallstätter Glacier, Minerals 13 (2023) 530.

[69] L. Retterath, P. Kohns, G. Ankerhold, Surface hardness imaging of a low-alloy steel using laser-induced breakdown spectroscopy, Spectrochimica Acta Part B: Atomic Spectroscopy 219 (2024) 107003. https://doi.org/10.1016/j.sab.2024.107003.

[70] E. Focus, M.J. Rwiza, N.K. Mohammed, F.P. Banzi, Health Risk Assessment of Trace Elements in Soil for People Living and Working in a Mining Area, Journal of Environmental and Public Health 2021 (2021) 1–10. https://doi.org/10.1155/2021/9976048.

[71] L. Quackatz, A. Griesche, J. Nietzke, T. Kannengiesser, In situ measurement of hydrogen concentration in steel using laser-induced breakdown spectroscopy (LIBS), Weld World 68 (2024) 915–923. https://doi.org/10.1007/s40194-023-01677-2.

[72] M. Sweeney, V. Etyemezian, T. Macpherson, W. Nickling, J. Gillies, G. Nikolich, E. McDonald, Comparison of PI-SWERL with dust emission measurements from a straight-line field wind tunnel, J. Geophys. Res. 113 (2008) 2007JF000830. https://doi.org/10.1029/2007JF000830.

[73] V. Etyemezian, J.A. Gillies, M. Shinoda, G. Nikolich, J. King, A.R. Bardis, Accounting for surface roughness on measurements conducted with PI-SWERL: Evaluation of a subjective visual approach and a photogrammetric technique, Aeolian Research 13 (2014) 35–50.

[74] J. Zhong, S. Wang, T. Qu, Undrained vane shear strength of sand-foam mixtures subjected to different shear rates, Journal of Rock Mechanics and Geotechnical Engineering 15 (2023) 1591–1602.

[75] S. Robinson, M.J. Brown, H. Matsui, A. Brennan, C. Augarde, W. Coombs, M. Cortis, A cone penetration test (CPT) approach to cable plough performance prediction based upon centrifuge model testing, Can. Geotech. J. 58 (2021) 1466–1477. https://doi.org/10.1139/cgj-2020-0366.

[76] D.Z. Yankelevsky, V.R. Feldgun, Y.S. Karinski, The false nose shape in a high velocity projectile penetration into dry sand, International Journal of Impact Engineering 177 (2023) 104492.

[77] M.A. Rice, B.B. Willetts, I.K. McEWAN, WIND EROSION OF CRUSTED SOIL SEDIMENTS, Earth Surf. Process. Landforms 21 (1996) 279–293. https://doi.org/10.1002/(SICI)1096-9837(199603)21:3<279::AID-ESP633>3.0.CO;2-A.